https://doi.org/10.5194/egusphere-2025-5750
Preprint. Discussion started: 19 January 2026

Seasonal to decadal evolution of firn properties and impacts on hydrology of the Juneau Icefield

Annika N. Horlings[1,2], Juliana Ruef[1,2], C. Max Stevens[3], Mikaila Mannello[4,5], Keegan Bellamy[4, 5], Tahi Wiggins[4, 5], Bradley Markle[1, 2], and Seth Campbell[4, 5]

[1]Institute of Arctic and Alpine Research, University of Colorado Boulder, Boulder, USA, 80301
[2]Department of Geological Sciences, University of Colorado Boulder, Boulder, USA, 80301
[3]Cryospheric Sciences Laboratory, NASA Goddard Space Flight Center, Greenbelt, MD, USA
[4]School of Earth and Climate Sciences, University of Maine, Orono, USA, 04469
[5]Climate Change Institute, University of Maine, Orono, USA, 04469

Correspondence: Annika N. Horlings (annika.horlings@colorado.edu)

Abstract. Alpine glaciers of Alaska are a significant contributor to global sea-level rise. Most Alaskan glaciers lose mass through surface melting due to increasing atmospheric temperatures, which may change regional glacier hydrology, including firn properties and the firn's capacity for meltwater retention. Here, we use field observations and firn modeling to investigate seasonal to decadal changes in the thermal and physical properties of firn on the Juneau Icefield, Alaska, and the impacts on the firn's capacity for meltwater retention. Firstly, we find that mean density and liquid water content generally increase up to 5% and 71 %, respectively, through the 2024 summer season, which suggests seasonal transient retention of meltwater in the snow and firn. Second, we find that modeled firn-air content from 1980-2019 decreased between 22% to 35% due to decreasing firn thickness and increasing firn density. Third, modeled results show that decreasing firn cold content caused increasing meltwater runoff from the firn (63% to 76%), decreased meltwater refreeze (-24 to -39%), and shift of the refreeze and runoff transition 7-18 days earlier in the season from 1980-2019 due to increasing surface melt and decreasing snow accumulation. Our results suggest that firn on the Juneau Icefield and other temperate alpine glaciers of Alaska will continue to lose long-term meltwater refreezing capacity. Further, inter-seasonal shifts in liquid water retention on these glaciers may introduce uncertainties in mass-balance calculations for sea-level rise estimates.

1 Introduction

1.1 Background

The alpine glaciers of Alaska constitute some of the most rapidly changing parts of the Earth's cryosphere. Collectively, Alaskan glaciers contribute 25% of the global land-ice loss to sea-level rise and comprise 38% of worldwide alpine glaciers that are currently thinning at an accelerating rate (Hugonnet et al., 2021). With continued atmospheric warming as a result of anthropogenic climate change, Alaskan glaciers are expected to remain a principal contributor to global sea-level rise at least through the end of the century (Fox-Kemper et al., 2021). By 2100, it is estimated that approximately 30% of glacier ice in

https://doi.org/10.5194/egusphere-2025-5750
Preprint. Discussion started: 19 January 2026

Alaska will have vanished and contributed to 17 ± 4mm of global sea-level rise under emission scenario RCP 4.5, relative to 2015 (Hock et al., 2019).

Most Alaskan glacier mass loss occurs through surface melting (Larsen et al., 2015). One critical connection between the surface and englacial or subglacial hydrological environment of a glacier is the firn. Firn influences the speed and volume of meltwater flow through a glacier, as well as its geochemical composition (The Firn Symposium Team, 2024; Fountain, 1996). Warming atmospheric temperatures and increasing surface melt may change regional glacier hydrology, including properties of the firn (i.e., the permeable and porous material from which snow transitions into glacier ice) and the firn's capacity to retain meltwater. On a broader level, understanding firn hydrology is fundamental to characterizing glacier dynamics and glacier-mass balance, which may potentially impact the glacier's contribution to sea-level rise, downstream ecology, and regional water resources (The Firn Symposium Team, 2024). However, the transit of surface meltwater through the firn remains understudied (The Firn Symposium Team, 2024; Vandecrux et al., 2020), especially in high-melt and high-accumulation temperate alpine glaciers of Alaska (Stevens et al., 2024), where most or all of the accumulation zone is located in the wet-snow zone (i.e., which is characterized by warm snow and some degree of runoff). As a result, our understanding of the physics, volume, and timescales of meltwater retention and runoff from the firn at these sites remains incomplete.

Here, we use a variety of field measurements (stratigraphy, density, liquid water content, and ground-penetrating radar), climate reanalysis, and firn modeling to investigate changes in firn properties over seasonal to decadal scales. We focus our study on the evolution of firn hydrology on one Alaskan glacier system: the Juneau Icefield in the Lingít Aaní (i.e., Tlingit land in southeast Alaska and northwest British Columbia).

1.2 Firn Hydrology

The current paradigm of firn hydrology is that meltwater flow through the snow and firn, driven by gravity and surface-tension gradients, occurs vertically (e.g, through a uniform wetting front or through preferential flow paths, depending on climatic and subsurface conditions) or laterally along stratigraphic transitions (Moser et al., 2024; Hirashima et al., 2019; Clerx et al., 2022). Surface melt that infiltrates firn may be refrozen in ice layers; may be retained through the irreducible water content; may be temporarily stored in seasonal or perennial features known as firn aquifers; and/or may drain to the englacial system or glacier bed via crevasses or moulins. Ultimately, meltwater may discharge to downstream environments with varying temporal lags that are in part dependent on firn properties (Colbeck, 1974; Forster et al., 2014; Poinar et al., 2017; Culberg et al., 2021).

The timing and rate of meltwater transit through the firn layer, including retention and runoff, is dependent on the thermal and structural (permeability) properties of the firn, which have been investigated through a variety of studies using in-situ data, geophysical observations, and modeling (Humphrey et al., 2021; Fountain, 1989; Forster et al., 2014; Ashmore et al., 2020; Culberg et al., 2021; Shadab et al., 2024). These properties include: (1) the amount of meltwater that infiltrates into the firn, which introduces latent heat; (2) the amount of cold content (i.e., the energy required to bring the firn to melting temperature) in the firn available to refreeze meltwater that has been introduced; (3) the pore space available to hold meltwater in the firn (Vandecrux et al., 2020; Humphrey et al., 2021), (4) structural (bulk and microstructural) heterogeneities which impact

https://doi.org/10.5194/egusphere-2025-5750
Preprint. Discussion started: 19 January 2026

permeability (McDowell et al., 2023; Machguth et al., 2016); and (5) the interplay of permeability and slope angle (i.e., on steeper slopes/higher permeability, water can move laterally more easily).

Refreeze of meltwater occurs when the cold content of the snow and firn is equal or exceeds the amount of latent heat held within the melt. At the summer-winter transition, lowering firn temperatures may refreeze the irreducible water leftover in the firn (Schneider and Jansson, 2004). In addition, following high-melt seasons, structural changes from ice-layer formation may reform the near-surface hydrological network in the accumulation zone. For example, ice layers and ice slabs may section off portions of the deeper firn and release latent heat during formation, making them an important part of firn hydrology and thermal balance (Culberg et al. (2021); Machguth et al. (2016)). These structural changes influence subsequent interactions and responses of the firn to surface melting and densification processes, limiting deeper pore space from melt infiltration, funneling meltwater along gradients, and/or priming firn for firn-aquifer formation through latent-heat release (e.g., Culberg et al. (2021)).

Further, firn aquifers form in regions of alpine glaciers and polar ice sheets with high summer surface melt (approximately $> 0.24 – 0.65$ m yr^{-1} w.e.) and high winter snow accumulation (approximately > 0.8 m w.e. yr^{-1}) (Forster et al., 2014; Miller et al., 2020). Firn may warm either by meltwater infiltration or through refreezing, which promotes latent-heat exchange. Then, firn-aquifer formation may occur if thermal energy from local meltwater recharge balances or exceeds the thermal energy lost from the aquifer (i.e., from winter sub-freezing temperatures), or drainage into crevasses (Miller et al., 2020). Formation and expansion of firn aquifers has been observed in the Arctic, due to atmospheric warming and increasing melt (Ochwat et al., 2021; Horlings et al., 2022; Kindstedt et al., 2025). Firn aquifers therefore may be increasingly important to broad-scale glacier behavior and mass balance because they may promote meltwater retention in the firn and prevent immediate runoff; store mass within the glacier; drain through crevasses that supply water to the bed; and/or may dampen downstream velocity variations and can change the seasonal behavior of the hydrological system (Miller et al., 2020; Poinar et al., 2017).

In addition, the efficiency and timing of runoff is influenced by the thermal, microstructural, and macrostructural properties of the snow and firn. Water exceeding the irreducible water content that could not percolate downward is available for runoff. The irreducible water content is the residual portion of water that is retained in the pore space of the firn due to capillary forces, and is approximately 6-8% water saturation or 2-3% of unit volume (Schneider and Jansson, 2004; Colbeck, 1974). Runoff of meltwater from the firn may be promoted by refreezing processes such as ice-layer formation, which may reduce or impede vertical percolation, increase lateral flow along the ice-layer surface into crevasses, and reduce the retention capacity of the firn (Machguth et al., 2016; Culberg et al., 2021).

On many alpine glaciers in Alaska, firn volumes have decreased as atmospheric warming has increased (Mannello, 2023; Larsen et al., 2015). However, few studies have focused on characterizing firn properties and hydrology within (1) the wet-snow zone; (2) temperate alpine glaciers that have warm temperatures, high-melt rates, and high snow-accumulation rates; and (3) even fewer on Alaskan glaciers with accumulation zone that are located in the wet-snow zone with those climate conditions (Machguth et al., 2023; Fountain, 1989; Stevens et al., 2024). Recent studies call for increased research on these Alaskan glaciers to understand firn hydrology, as well as other glaciological applications such as the improvement of firn-densification models and geodetic mass-balance calculations (Stevens et al., 2024). We must better understand how atmospheric warming

https://doi.org/10.5194/egusphere-2025-5750
Preprint. Discussion started: 19 January 2026

and increasing surface melt are changing firn hydrology, including firn properties, capacity for meltwater retention, and timing of meltwater runoff in high-melt and high-accumulation alpine environments such as those found in Alaska.

1.3 The Juneau Icefield

In this study, we investigate the evolution of firn hydrology on the Juneau Icefield, an interconnected glacier system that consists of a large low-slope plateau of over 1050 glaciers (as of 2019) drained by 40 outlet glaciers in the Coast Range of Lingít Aaní (southeast Alaska/northwest British Columbia) (Davies et al., 2022). The icefield predominantly has a temperate maritime climate with abundant snowfall, temperate conditions, and rainfall during the summer; the eastern icefield is characterized by a drier continental climate. The Juneau Icefield may be particularly vulnerable to climate change due to an interplay of increasing ELAs, albedo, and thinning rates which have led to accelerating ice loss, especially since 2005 (Hock et al., 2019; Davies et al., 2024). The icefield is projected to lose significant mass in the coming decades (Ziemen et al., 2016).

The Juneau Icefield has an expansive accumulation area in the north (>1500 m elevation) and in the south (> 1200 m elevation), which has been decreasing in area as equilibrium-line altitudes increase due to melt, albedo, and hypsometrically controlled ablation feedbacks (Davies et al., 2024). Across the accumulation zone, the Juneau Icefield suffered significant loss of firn volume in recent decades (Mannello, 2023). While firn volumes and therefore available porosity is decreasing on the icefield, we expect that the limiting factor on the volume of melt that can refreeze in the firn is the cold content (i.e., the energy required to warm the firn to the melting point).

Here, we motivate this study through the following questions: (1) how are melt and thermal properties (i.e., capacity for refreezing) of the firn changing over seasonal to decadal scales on Alaskan glaciers? and (2) how are firn changes impacting hydrology? We hypothesize that the firn has been thinning and warming due to increasing wintertime temperatures and increasing melt, which may decrease meltwater retention and shift seasonal timing depending on site location and specific melt events. We use three modes of investigation to begin to explore this question: field measurements, climate reanalysis, and firn modeling. We collected field measurements (including density, liquid-water content, and stratigraphy) on the Juneau Icefield, Alaska during June and July 2024 to primarily investigate short-term changes in firn properties. We analyze climate reanalysis products (Ing et al., 2025) to determine changes in surface forcing important to firn densification and evolution. Finally, we simulated the evolution of firn properties (including density, liquid-water content, and retention/runoff) over decadal scales using the Community Firn Model (Stevens et al., 2020) and compared the results to our recent observations.

2 Methods

2.1 Field measurements

2.1.1 Firn cores

We retrieved 13 firn cores at four different sites on the Juneau Icefield over the period June 2 - July 25, 2024: a site at the divide of the Matthes and Llewellyn Glaciers (MLD); at the intersection of the Matthes and Gilkey Glaciers (MG3); at the Northwest

https://doi.org/10.5194/egusphere-2025-5750
Preprint. Discussion started: 19 January 2026

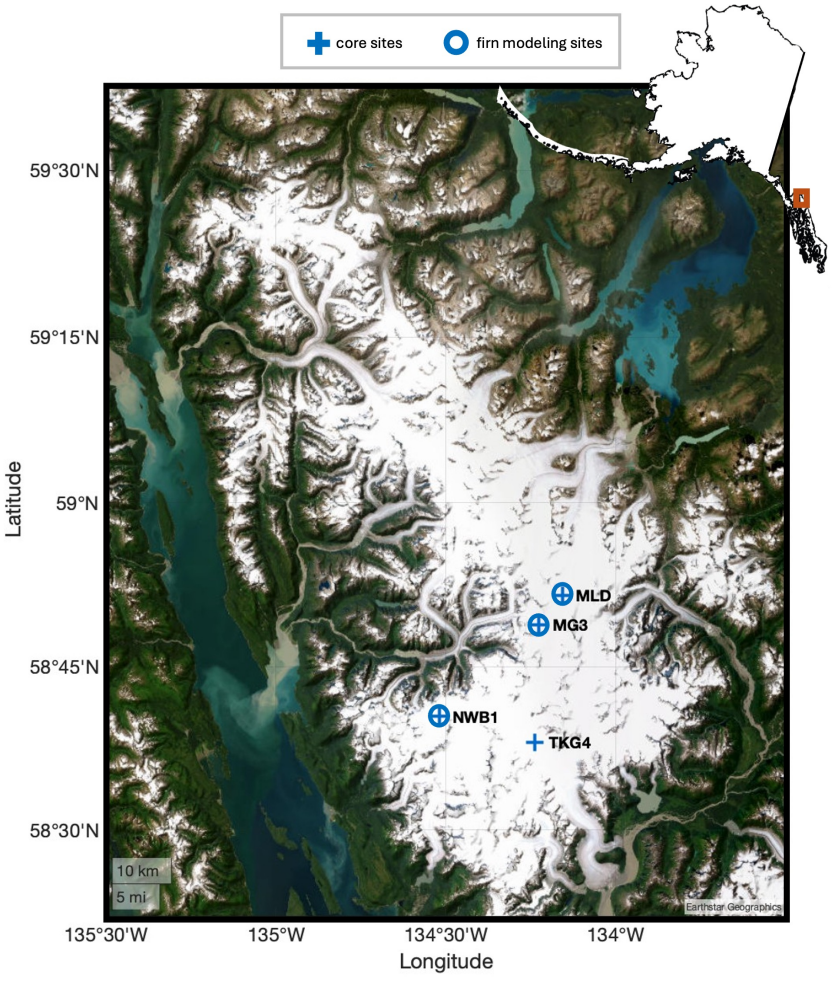

Figure 1. Overview map of the Juneau Icefield, and the four sites situated along the Taku Glacier, including the tributary Matthes Glacier and Northwest Branch, that are the focus of this study. Core sites are represented by the blue crosses (MLD, MG3, NWB1, and TKG4). Sites that are in the accumulation zone and that we ran the Community Firn Model for are represented by the blue cross and blue circle (MLD, MG3, and NWB1). Brown rectangle represents the region on the larger Alaska map. Main map is derived from the Randolph Glacier Inventory (Consortium et al., 2023).

120 Branch of the Taku Glacier (NWB1); and at a firn-covered site in the current ablation zone of the Taku Glacier (TKG4). These include different climatic regimes (e.g., different altitudes, proximity to the coast, and surface mass balance) (Figure 1; Table 1) and their history of previous repeat mass balance and snow density measurements (McNeil et al., 2020). The site with the highest elevation is MLD; with the closest marine proximity is NWB1; with the highest snow-accumulation rates is NWB1;

https://doi.org/10.5194/egusphere-2025-5750
Preprint. Discussion started: 19 January 2026

Table 1. Site descriptions for all sites. Marine proximity is defined as closest distance to the Pacific Ocean.

	MLD	MG3	NWB1	TKG4
Elevation (m)	1900	1780	1500	1120
Marine Proximity (km)	165	160	140	150

with the lowest melt rates is MLD; and with the lowest snow-accumulation rates/highest melt rates is TKG4. MLD, MG3, and NWB1 sites are located in the wet-snow zone; TKG4 is located in the ablation zone. In the results, we discuss climate analyses and firn modeling at the three sites in the accumulation zone only.

We drilled the firn cores with a FELICS 2-inch ice-core drill powered by a portable Honda generator and collected repeat cores at all sites (Table 1). Additionally, to measure surface-melt rates, we set an ablation stake at each site and recorded surface snow height at the time each firn core was taken. Each repeat firn core at a site was taken within 1-2 m of each other.

2.1.2 Stratigraphy

We recorded the stratigraphy of each firn core, including ice-lens depth in the core, ice-lens continuity, and ice-lens width; qualitative grain-size changes; snow-firn transition; and presence of liquid water. We attribute uncertainty in the stratigraphic record to the accuracy of the ruler and subjectivity of human identification of the features. We report all layer depths to 1-cm accuracy and relative to the first core's summer snow surface at the site (i.e., accounting for ablation of the surface), as other reference depths such as the previous summer surface were difficult to discern within the cores and because the firn-ice transition was not reached for all cores.

2.1.3 Density

We also obtain density for sections of the firn cores, from mass (weighing the core samples) and volume (knowing the core length and diameter). Sections were partitioned every 20 cm except in cases where natural breaks or ice lenses occurred. We report all depths associated with the density measurements relative to the first core's snow surface at the site. We follow Ochwat et al. (2021) and Kindstedt et al. (2025) to assess density and its uncertainties, where density is defined in terms of mass m and volume V:

$$\rho = \frac{m}{V}, \tag{1}$$

where $V = f\pi L\left(\frac{D}{2}\right)^2$, f is defined as the subjective quantity of 'cylindrical completeness' (0-1) (e.g., Ochwat et al., 2021), L is the core-segment length, and D is the diameter. Uncertainty in the density measurements can be quantified through random and systematic uncertainties in mass and volume, per propagation of uncertainties:

$$d\rho = \rho\sqrt{\left(\frac{dm}{m}\right)^2 + \left(\frac{dV}{V}\right)^2} \tag{2}$$

https://doi.org/10.5194/egusphere-2025-5750
Preprint. Discussion started: 19 January 2026

and

$$dV = V\sqrt{\left(\frac{df}{f}\right)^2 + \left(\frac{dA}{A}\right)^2 + \left(\frac{dL}{L}\right)^2} \tag{3}$$

where $dA = \pi D\frac{dD}{2}$; $dL = dD = 0.25$ cm (for rough and/or crumbly edges of the firn core); $df = 0.1$ for $f = 0.8$ and $df = 0.2$ for $f < 0.8$ (to account for more challenging visual inspection of less complete core samples, following Ochwat et al., 2021).

We use repeat firn cores to examine how the mean density of the firn changes through the summer season. We calculate mean density based on comparing common parts of the firn cores, i.e., those that did not ablate away subsequently, or those that are within a common depth range after considering ablation. Because we did not take ablation-stake measurements at MG3, we are unable to calculate mean density changes at that site.

2.1.4 Liquid Water Content

We used an A2 Photonics WISe sensor (e.g., Webb et al. (2021)) to calculate liquid water content (LWC) in the snow and firn, sampled at approximately 20-cm spacing on the firn cores on samples with no ice lenses. The WISe sensor samples a 325 cm^3 volume and has a marked uncertainty of 1 % vol liquid water content. The sensor measures dielectric permittivity of the snow or firn, the property which characterizes the degree of electrical polarization experienced by a material when exposed to an external electric field. We use equation 4 to convert permittivity (k) to volumetric liquid water content (θ_w) (Webb et al., 2021):

$$k = \left[1.0 + 0.0014(\rho_s - 1000\theta_w) + 2 \times 10^{-7}(\rho_s - 1000\theta_w)^2\right] + (0.01\theta_w + 0.4\theta_w^2)k_w \tag{4}$$

where ρ_s is density; k_w is the relative permittivity of liquid water at 0 degree Celsius; and the background impact of dry snow permittivity is the bracketed part of the equation. For these calculations, we use measured density for ρ_s because of the availability of concurrent permittivity and density measurements and the uncertainty associated with the inability to measure dry density prior to melt onset. We do this with the understanding that this may positively bias our LWC calculations.

We also calculate mean LWC for repeat firn cores, and consider comparable parts of the firn core given measurements of ablation and core length. Due to the lack of ablation-stake measurements at MG3, we are unable to calculate mean liquid water content changes at that site (i.e., we cannot know the common depth range shared by the repeat cores). Note that our LWC values are reported in percent volume (defined as the volumetric percentage of total volume of the material), and not water saturation (defined as the amount of pore space occupied by liquid water).

2.1.5 Ground-penetrating Radar

To determine the continuity of major ice layers around the firn-core sites, we used ground-penetrating radar (GPR). We collected GPR data with a 400 MHz Geophysical Survey Systems Incorporated (GSSI) Model 50400S antenna and GSSI SIR-4000

https://doi.org/10.5194/egusphere-2025-5750
Preprint. Discussion started: 19 January 2026

paired with a Garmin GPSMAP 79s at 300-350 ns with 2048 samples per trace. The GPR was mounted on a Siglin sled and towed by a snowmachine, traveling at approximately 8-10 km hr^{-1}, to image the snow and firn (approximately 30-m depth). The grid GPR data were collected the same day as firn-core drilling, though not always collected while firn core drilling was in progress.

We processed the GPR data using ImpDAR, an open-source impulse radar processing and interpretation toolbox (Lilien et al., 2020). We applied a vertical bandpass (100-800 MHz) filter and a time-zero correction, clipped stationary periods, applied constant spacing, and applied a horizontal bandpass averaged over 100 scans. A normal move-out correction was applied and firn-density profiles were incorporated into the time-to-depth conversion to determine layer depths. We also tracked the surface and distinct reflectors signifying ice layers across the radar grids.

2.2 Climate Reanalysis

We determine magnitude and trends in climate variables (including temperature, surface snow melt, snow accumulation, and rainfall) for our four study sites covering the dates between 1980 to 2019 using modeled surface mass balance (SMB) data from Ing et al. (2025). Ing et al. (2025) simulated historical and future SMB for the Juneau Icefield by forcing the COupled Snowpack and Ice surface energy and mass-balance model in Python (COSIPY) with three different climate reanalyses. Of those, we use the results from The Climate Forecast System Reanalysis (CFSR) (Saha et al., 2010). We use the CFSR climate output from Ing et al. (2025) to determine interannual and daily variability and trends in climate variables, and as input to the Community Firn Model. Spatial resolution is 0.01° latitude and longitude, and temporal resolution is daily.

2.3 The Community Firn Model

We use the Community Firn Model (CFM) to simulate firn evolution on the Juneau Icefield. The CFM is an open-source, modular model framework that is designed to simulate the evolution of a variety of firn properties including density, compaction rate, temperature, liquid water content, runoff and refreezing, and it includes 13 firn models in its published form (Stevens et al., 2020). The CFM uses a one-dimensional Lagrangian framework to track the properties of firn parcels as they compact from the surface into glacier ice. Boundary conditions as input to the model include snow-accumulation rate, skin temperature, and surface-snow density, as well as others that may be required for varying firn models.

We simulate the evolution of firn density, temperature, liquid-water content, and melt runoff and refreezing from 1980 - 2024 with the Kuipers Munneke et al. (2015) densification equations implemented with a bucket meltwater percolation scheme. We choose the Kuipers Munneke et al. (2015) densification equations because they were developed to simulate firn densification in north and central Greenland and are often used for melt-affected areas.

Bucket schemes implemented in firn-densification models are one of many treatments of meltwater retention and flow within water-saturated firn layers. In bucket schemes, water may percolate downward when the water exceeds the capillary capacity of the firn parcel and will stop either when the water reaches a firn parcel that has enough cold content and pore space for refreezing, or when there is an impermeable layer such as an ice layer and the meltwater runs off (The Firn Symposium Team, 2024). The remaining water from each parcel will continue to percolate to the subsequently deeper parcel until all water is

https://doi.org/10.5194/egusphere-2025-5750
Preprint. Discussion started: 19 January 2026

refrozen or runoff. In the model, we define the irreducible water content as dependent on the dry density following Coléou and Lesaffre (1998). While there are limitations with using bucket meltwater percolation schemes, currently, more complex models do not reliably model firn meltwater processes better than approaches that use a simple bucket scheme (Vandecrux et al., 2020).

We force the CFM with CSFR climate data from 1980-2019 Figure 2 and surface density of 350 kg m^3. We spin up the model using a repeating climate routine implemented from 1831-1980 (i.e., repeating the 1981-1990 climate over and over again, so that there is variability in the spin up climate). We run the model with one-day timesteps and output firn density, temperature, firn thickness, depth-integrated porosity (i.e., firn-air content), melt volume, refreeze, runoff, and liquid-water content.

Further, we quantify the cold content, a key parameter in defining the firn's meltwater refreezing capacity. Cold content is the energy necessary to heat the firn to the melting temperature. We define the cold content and latent heat for the upper 20 m of the firn column following (Culberg et al., 2021):

$$CC = c \int_{z=20m}^{z=0m} rho_j (T_j - T_{melt})\, dz_j. \tag{5}$$

3 Results

3.1 Changes in climate

We examine snow accumulation, skin temperature, snow melt, and rainfall at the three study sites in the accumulation zone (MLD, MG3, NWB1) for 1980-2019 (Table 1; Figure 2). At MLD, MG3, and NWB1, mean annual surface temperature range from -4.6 to -6.0 °C, and increased at a rate of 0.16-0.22 °C per decade from 1980-2019. Mean values of the cumulative annual snow accumulation range from 2.4 to 2.9 m i.e. a^{-1} for MLD, MG3, and NWB1, and decreased at -0.11 to -0.16 m i.e. a^{-1} per decade from 1980-2019. The mean cumulative annual surface-snow melt ranges from 0.92 to 1.5 m i.e. a^{-1} for MLD, MG3, and NWB1, respectively, and increased 0.11 to 0.26 m i.e. a^{-1} decade $^{-1}$ from 1980-2019. Mean cumulative annual rainfall ranges from 0.15 to 0.46 m i.e. a^{-1} with little long-term change.

We also compare annual cumulative melt and annual cumulative rain to cumulative snow accumulation (Figure A**??**). From 1980-2019, we find that the melt to snow accumulation ratio increases at 0.23-0.45 per decade; that the melt and rain to snow accumulation ratio increases at 0.43-0.65 per decade; and the rain to accumulation ratio decreases at -0.11 to -0.12 per decade.

We also calculate high-melt years, defined as a year that exceeds one standard deviation above the mean annual melt. For MLD, there are 6 high-melt years (1989, 2009, 2013, 2016, and 2019); for MG3, there are 7 high-melt years (1989, 1990, 2004, 2009, 2013, 2015, and 2019); and for NWB1, there are 8 high-melt years (1989, 1990, 1993, 2004, 2009, 2013, 2016, and 2019). Most high-melt years have occurred within the last ten years of the interval, with 1989, 2009, 2013, and 2019 ubiquitous across the three sites.

Analysis of seasonal climate for all sites is shown in Table 2. Mean annual winter surface temperatures on the Juneau Icefield are increasing. Further, the onset of the melt season (defined here as the onset of five consecutive days with nonzero melt) is shifting earlier in the year: from 25 May to 14 May (MLD); 23 May to 14 May (MG3); and 3 May to 28 April (NWB).

https://doi.org/10.5194/egusphere-2025-5750
Preprint. Discussion started: 19 January 2026

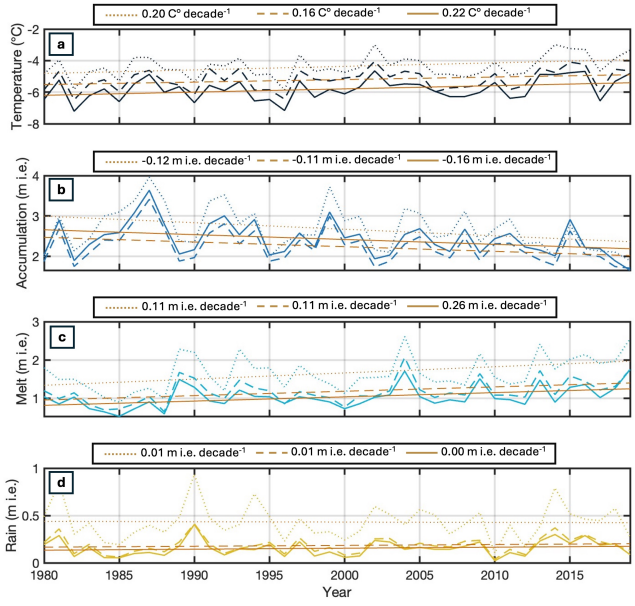

Figure 2. Annual climate at each site in the accumulation zone (MLD, dotted line; MG3, dashed line; NWB1, solid line) from the product by Ing et al. (2024): a) mean annual skin temperature, b) cumulative annual snow-accumulation, c) cumulative surface melt, and d) cumulative rainfall.

Table 2. Mean climate variables over 1980-2019, and changes in climate variables for the three accumulation-zone sites in this study: MLD, MG3, and NWB1, derived from Ing et al. (2025).

	MLD	MG3	NWB1
Surface temperature (°C)	-6.0 ± 0.6	-5.4 ± 0.6	-4.6 ± 0.6
Snow accumulation (m i.e. a^{-1})	2.6 ± 0.5	2.4 ± 0.4	2.9 ± 0.5
Melt rate (m i.e. a^{-1})	0.9 ± 0.3	1.1 ± 0.3	1.5 ± 0.5
Rainfall rate (m i.e. a^{-1})	0.2 ± 0.1	0.2 ± 0.1	0.5 ± 0.2
M:A ratio	0.4 ± 0.2	0.5 ± 0.2	0.7 ± 0.2
(M+R):A ratio	0.5 ± 0.2	0.6 ± 0.2	0.8 ± 0.3
High-melt years	6	7	8
Winter temperature increase (°C per decade)	0.3	0.2	0.3
Shift in melt-season onset (days per decade)	+ 2.8	+ 2.3	+ 1.3
Increase in melt days above sd (days per decade)	3.3	2.5	6.3
Lengthening of melt season (days per decade)	5.8	3.8	4.3

https://doi.org/10.5194/egusphere-2025-5750
Preprint. Discussion started: 19 January 2026

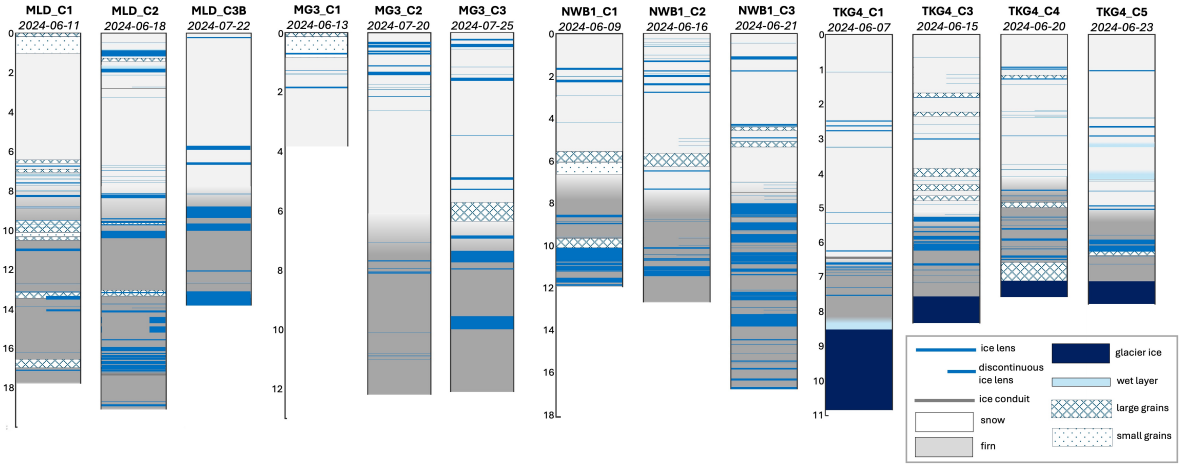

Figure 3. Stratigraphy of the repeat firn cores at sites MLD, MG3, NWB1, and TKG4. All surfaces are corrected for ablation, except MG3, where no ablation measurements exist. Repeat cores were taken within 1-3 m of each other. The differences in stratigraphy show that even great local variability exists in high-melt and highly temperate snow and firn. Large volumes of liquid water were found at the base of the TKG4_C1 core.

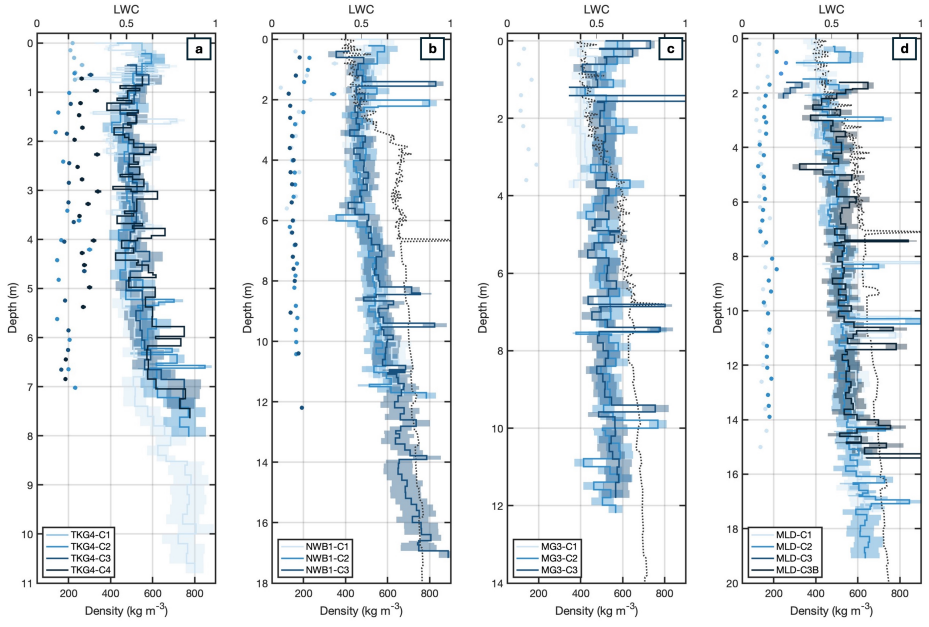

Figure 4. Measured density (blue lines), modeled depth-density profile for 1 June 2019 (dotted black line), measured liquid water content (blue circles), and uncertainty estimates (shaded region) at the four sites. a) Site TKG4; b) Site NWB1; c) Site MG3; d) Site MLD.

https://doi.org/10.5194/egusphere-2025-5750
Preprint. Discussion started: 19 January 2026

The length of the melt season has consequently lengthened, from 106 to 129 days (MLD); 115 to 130 days (MG3); and from approximately 138 to 155 days (NWB1). The intensity of melt is also increasing at all sites, where the number of "melt events" (we define days with melt > 0.5 mm yr^{-1}) also increased: 104 to 117 days (MLD); 119 to 129 days (MG3); and approximately 127 to 152 days (NWB1).

3.2 Field Measurements

We examine changes in the firn cores in an Eulerian framework, accounting for ablation as well as core length in order to make accurate comparisons.

3.2.1 Density

Densities for all repeat cores at the four sites are shown in Figure 4. Densities vary due to ice layers, liquid water, and differences in snow and firn dry density. Mean density for all firn cores through the 2024 summer are shown in Table 3. Note that mean densities also include both liquid and solid phases. Increases in mass occur at all sites over the season but do not increase linearly or monotonically: 4.6% increase at MLD, 1.1% increase at NWB; and 1.8% increase at TKG4. We note that some of the mean density changes observed between repeat firn cores are within the uncertainty range. Mean densities remain similar, within uncertainty bounds, in the first two cores at MLD and TKG4, while decrease between NWB1 core 1 and core 2. All mean densities increase subsequently.

3.2.2 Liquid Water Content

The measured volumetric liquid-water content (LWC) generally range from 10 to 30 % vol. at all measurement sites (Figure 4). LWC measurements were collected approximately every other sample in the core (approximately 40 cm depth spacing) and were collected until the density became too high (approximately 550 kg m^{-3}) and the WISe sensor could not be inserted into the sample. No LWC measurements were obtained in July due to a limited time in the field.

Mean LWC generally increases for the core section we compared, but changes non-monotonically through the season (Table 3): 27% increase at MLD; 71% increase at NWB; and 46.4% increase at TKG4. Site TKG4 had generally the highest LWC of all sites (> 17 % vol. mean LWC for the core, with highest measurements at 34 % vol.). Liquid water was found at the base of TKG4-C1 (not shown), but was not found during subsequent sampling and we did not take WISe-sensor measurements on that firn core. Site NWB1 had high LWC (up to 34 % vol.) near the surface but similar LWC to MLD at depth (approximately 7-14 % vol. mean LWC) and generally lower LWC than TKG4. For NWB1, mean LWC increases then decreases through the season. In contrast, LWC at MLD increased (by approximately 2-3 % vol.) between the two cores at all depths, especially in the upper 3-4 m. We only sampled firn LWC at MG3 (not plotted) once before the drill became stuck due to freezing. Total uncertainty of LWC measurements accounts for instrument errors (1 % vol.) and potential melting of the samples between recovery and measurement (which we designate as 2 % vol.).

https://doi.org/10.5194/egusphere-2025-5750
Preprint. Discussion started: 19 January 2026

Table 3. Changes in mean density and liquid-water content (LWC) for repeat firn cores taken at MLD, NWB1, and TKG4. Since ablation was not measured at MG3, we cannot accurately compare core sections and cannot calculate mean-density or LWC changes.

	Date	Mean Density (kg m^{-3})	Mean LWC (% vol)
MLD_C1	2024-06-11	520	8.9
MLD_C2	2024-06-18	519	11.3
MLD_C3	2024-07-22	544	–
NWB1_C1	2024-06-09	523	7.3
NWB1_C2	2024-06-16	504	14.3
NWB1_C3	2024-06-21	529	12.5
TKG4_C1	2024-06-07	543	16.8
TKG4_C3	2024-06-15	541	18.2
TKG4_C4	2024-06-20	553	24.6

3.2.3 Stratigraphy

Stratigraphy of all cores shows a mixture of ice lenses, ice layers, and some variation in grain size. Upon retrieval of one core (TKG4_C1), we encountered liquid water pooling at the base. Grain size was intermittently noted on the cores when significantly large or fine, and therefore we do not provide a detailed description of grain transitions.

In cores at MLD_C1 and MLD_C3, the upper 6 and 5 m, respectively, were mainly snow. In contrast, core MLD_C2 had two significant ice layers in the upper 2 m (up to 6 cm thick) and some smaller (0.25 cm) ice layers. At the snow-firn transition for each MLD core, there were a cluster of ice layers: small to large ice layers in MLD_C1 and MLD_C2 (0.25-3 cm thick), and larger (> 0.25 cm) ice layers in MLD_C3 (up to 11 cm thick). Large snow crystals occur above the snow-firn transition in MLD_C1. Below the snow-firn transition, core MLD_C1 had three ice layers (1-2) cm that were not clustered, and a multitude of hairline ice layers throughout. In contrast, core MLD_C2 has clusters of ice layers (1-2 cm and up to 8.5-cm in thickness) around 10-m in depth and 14-17-m in depth. Core MLD_C3 had thick ice layers (3-22 cm thick) clustered also around 10-m in depth. We cannot conclude the character of ice lenses at 14-17-m in depth because that is beyond the core depth.

In the upper 0 - 3 m of the snow of cores NWB_C1, NWB_C2, NWB_C3, there were smaller ice layers (0.25 cm-1 cm in C1; 0.25-2 in C2; and 0.25-3 cm in C3). Coarse snow grains existed above the snow-firn transition. Below the snow-firn transition, significant ice layers existed in cores NWB_C1, NWB_C2, NWB_C3 but with variable clustering and thickness. In core NWB_C1, many closely situated ice layers (up to 4.5 cm thick) were clustered from 10-12 m depth. In contrast, in core NWB_C2, several significant ice layer occurred at 11 m depth (up to 4-5.5 thick) but were less than core NWB_C2. Core NWB_C3 had the most ice layers, as significant ice layers existed between 8 and 14-m depth (up to 6 cm thick and multiple > 4 cm thick).

We identified some smaller ice layers (0.25 - 3 cm thick) in the snow of cores TKG4_C1, TKG4_C3, TKG4_C4, and TKG4_C5. In the snow of core TKG4_C5, from 3-5 m depth, we identified a 10-cm and 20-cm portion of liquid water

https://doi.org/10.5194/egusphere-2025-5750
Preprint. Discussion started: 19 January 2026

Table 4. Summary of modeled firn results from the Community Firn Model (Stevens et al., 2020) using the Kuipers Munneke firn model with a bucket scheme and irreducible water content defined by Coléou and Lesaffre (1998), forced with CSFR climate data from 1980-2019 derived from Ing et al. (2025).

	MLD	MG3	NWB1
Firn-thickness change 1980-2019	-16 % (-6.9 m)	-21 % (-8.9 m)	-27 % (-11.8 m)
Firn-thickness change 2012-2019	-11 % (-4.4 m)	-11 % (-4.1 m)	-19 % (-7.4 m)
Firn-air content change 1980-2019	-21 % (-3.1 m)	-27 % (-3.6 m)	-35 % (-4.9 m)
Refreeze change 1980-2019	-34 % (-0.03 m)	-22 % (-0.02 m)	-36 % (-0.03 m)
Runoff change 1980-2019	70 % (0.65 m)	55 % (0.56 m)	48 % (0.78 m)
Change in percent melt and rain that is refrozen	-58 %	-44 %	-52 %
Change in percent melt and rain that is runoff	8 %	12 %	12 %
Mean melt onset 1980-2019	May 11	May 8	May 3
Mean start of runoff season 1980-2019	June 22	June 18	June 17
Shift in start of runoff season 1980-2019 (days)	-19	-9	-18
Change in cold content 1980-2019	-48 %	-34 %	-39 %
Change in days per year with $\leq$ 0.05 MJ m^{-2} 1980-2019	+19 %	+15 %	+7 %

saturated snow. In TKG4_C1, we encountered liquid water spilling out of the base at and above the firn-ice transition. In the firn of TKG4_C1, a section of smaller ice layers (0.25-1 cm thick) occurred between 6 and 7.5 m. In TKG4_C4, a section of smaller ice lenses (0.25-3 cm) were present between 5 and 7 depth. A section of large ice layers (1 -5.5 m) occurred between 5-6.5 m depth in TKG4_C3, and between 6 and 7 m depth in TKG4_C5.

In MG3_C1 there were ice layers from 0-3 m in the snow in all repeat cores. In the upper 1 m of MG_C1, there is a 12-cm section of large crystals. In MG3_C2 and in MG3_C3, there are ice layers (0.25-4 cm) in the upper 2 m. In cores MG3_C2 and MG3_C3, there are significant ice layers (>0.25 cm) in the upper 3 m, whereas in MG3_C1 there are only hairline ice layers. Some smaller ice layers occur in the firn of MG3_C2 (1-2 cm thick), and in contrast, significant ice layers occur in the firn of MG3_C3 (up to 12.5 cm thick).

3.2.4 Ground-penetrating radar

At MLD, we identify the phase response at one of the strongest reflectors at approximxately 10 m depth. We observe a change in phase of this reflector relative to the direct wave (from +-+ to -+-) between the first and second core and radar collections, which indicates a change in layer properties. We also identify a decrease in amplitude at 10 m between the first and the second collections, which suggests a change in permittivity contrast and/or additional attenuation of the wave above 10 m. This coincides with the development of a thick section of ice layers (including a 10-cm ice layer) in the firn at a previously thick large-grained layer.

https://doi.org/10.5194/egusphere-2025-5750
Preprint. Discussion started: 19 January 2026

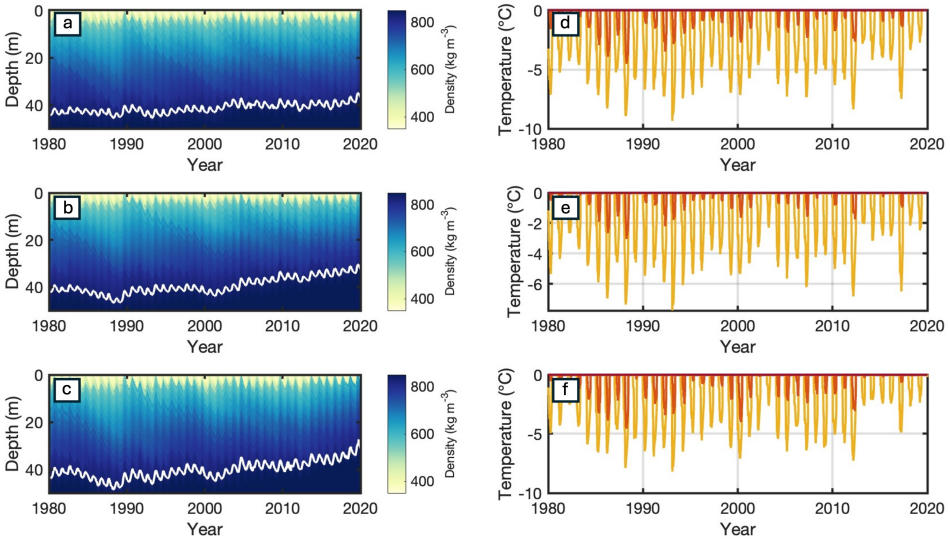

Figure 5. Modeled profiles of density and modeled firn temperature at 3-m depth (light orange), 5-m depth (dark orange), and 8-m depth (red - at 0 °C) through time from Kuipers Munneke (2015) firn-densification model at the MLD site (a and d); MG3 site (b and e); and NWB1 site (c and f).

3.3 Modeling results

To investigate changing firn properties over decadal timescales, we ran the Community Firn Model from 1980-2019.

Modeled bubble close-off depth decreases, ice-rich layers are introduced into the firn (Figure 4a-c), and modeled snow and firn temperatures increase from 1980-2019 (4d-f). Specifically, the 5-m temperature cools below 0 degrees during the winter season less frequently over the period at all sites.

Recent decrease in firn-column thickness (defined as the surface to bubble close-off depth) occurs at all three sites (Table 4; Figure 6): at MLD, 11% decrease between 2012-2019 and 16% decrease between 1980-2019; at MG3, 11% decrease between 2012-2019 and 21% decrease between 1980-2019; and at NWB1, a 19% decrease between 2012-2019 and 27 % decrease between 1980-2019. Firn-air content decreased by 21 % at MLD; 27 % at MG3; and 35 % at NWB1.

Annual refreeze in the firn is generally low and highly variable in time for all sites (Figure 7b), and overall decreased from 1980-2019 (34% for MLD; 22% for MG3; and 36% for NWB1, with a recent spike in annual refreeze in 2012 and 2017. Annual runoff (Figure 7c) in the firn increased from 1980-2019 (70% for MLD; 55% for MG3; and 48% for NWB1.

Further, the percent liquid water introduced into the firn that is refrozen is decreasing while runoff is increasing (Figure 8). From 1980-2019, the percentage of melt and rain that is refrozen in the firn decreased: for MLD, from 8 % to 3 %; for MG3, from 6 % to 3 %; for NWB1, from 3 % to 1.5 %. From 1980-2019, the percentage of melt and rain that is runoff in the firn increased: for MLD, from 82 % to 88.5 %; for MG3, from 77 % to 87 %; and for NWB1, from 75 - 84 %.

https://doi.org/10.5194/egusphere-2025-5750
Preprint. Discussion started: 19 January 2026

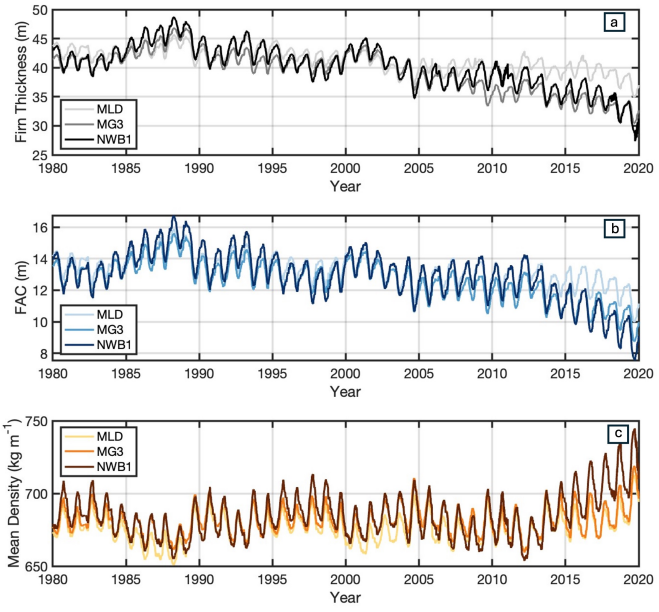

Figure 6. Modeled results from the Kuipers Munneke (2015) firn-densification model. a) Firn thickness; b) depth- integrate porosity; c) mean density of the full firn column down to bubble close-off depth

Model results also suggest that layers of LWC > 10 % vol is retained inter-annually at all sites (Figure A7): at or near bubble close-off for all sites, and in the shallow firn (0-20 m) at MLD and MG3 from 2008 - 2019 and at NWB1 from 1985-1990.

We define the onset of the melt season as 5 consecutive days of melt. The mean day of the melt-season onset is May 11 (MLD); May 8 (MG3); and May 3 (NWB1). Seasonally, there is a tradeoff between runoff and refreeze in the firn. The main transition between the firn refreeze and runoff season in spring is highly variable, with a mean onset of runoff of June 22 (MLD); June 18 (MG3); and June 17 (NWB1), with a shift earlier in the year by 19 days (MLD), 9 days (MG3), and 18 days (NWB1) from 1980-2019.

3.4 Cold content

We quantify the cold content in the upper 20 m of firn at MLD, MG3, and NWB1. Annual mean cold content decreased at all sites from 1980-2019 (Table 4), with a modeled -48% decrease (trend of -0.86 MJ m^{-2} per decade) at MLD; 34% decrease (trend of -0.57 MJ m^{-2} per decade) at MG3; and 38% decrease (trend of -0.73 MJ m^{-2} per decade) at NWB1. Winter (Nov 1 - April 30) cold content also decreased, a modeled -30 % decrease (with a trend of -1.02 MJ m^{-2} per decade) at MLD; -63 % (with a trend of -0.63 MJ m^{-2} per decade) at MG3; and -65 % (with a trend of -1.25 MJ m^{-2} per decade) at NWB1.

https://doi.org/10.5194/egusphere-2025-5750
Preprint. Discussion started: 19 January 2026

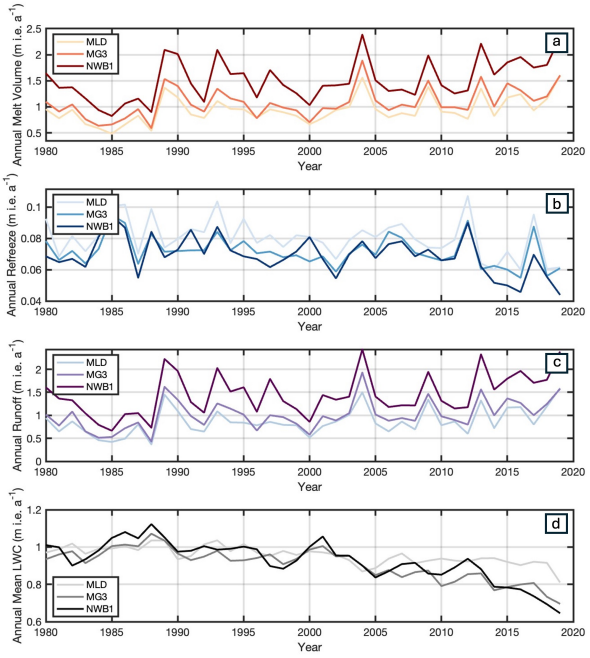

Figure 7. Model results of a) cumulative annual melt volume, b) cumulative annual refreeze in the firn, c) cumulative annual runoff, and d) mean annual LWC in the firn

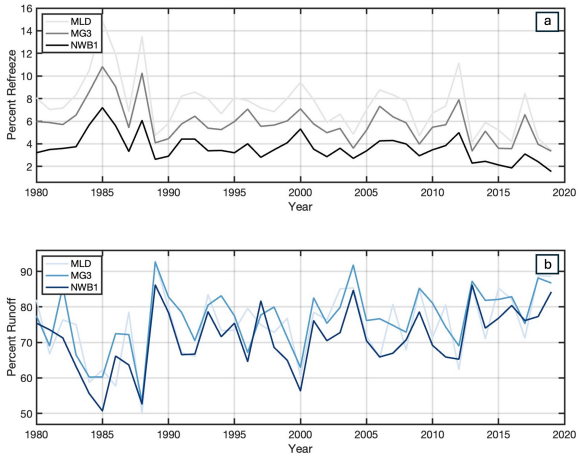

Figure 8. Model results of a) percent of annual melt and rain that refroze in the firn, and b) percent of annual melt and rain that ran off from the firn.

https://doi.org/10.5194/egusphere-2025-5750
Preprint. Discussion started: 19 January 2026

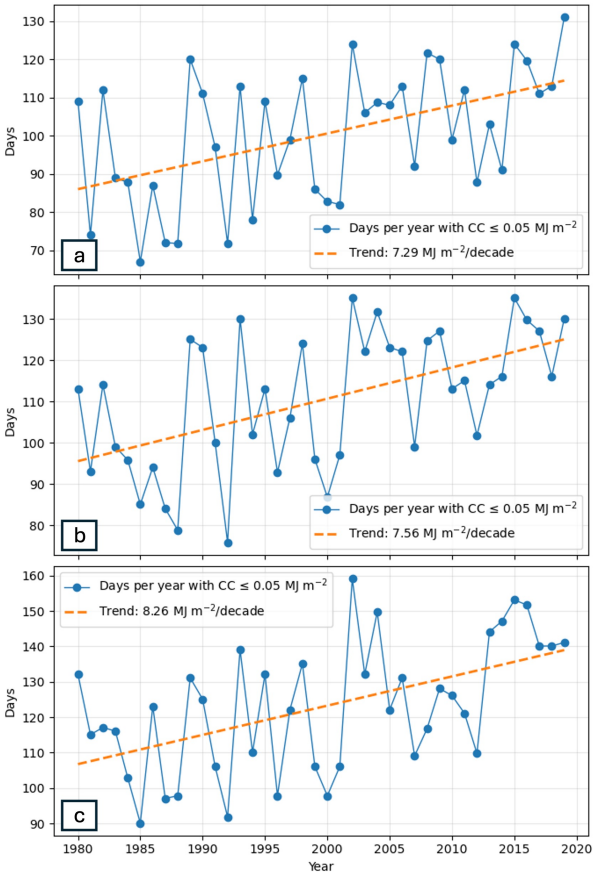

Figure 9. Number of days per year with cold content ≤ 0.05 MJ m^{-2} for a) MLD, b) MG3, and c) NWB1, derived from the modeled results.

Consequently, the number of days with cold content ≤ 0.05 MJ m^{-2} is increasing (which means less days with enough latent heat to refreeze meltwater): 5.3 days per decade (MLD); 4.3 days per decade (MG3); and 2.3 days per decade (NWB1).

4 Discussion

In the following sections, we address the central questions motivating this study:

1) How are the thermal and physical properties of the firn changing on seasonal to decadal scales on the Juneau Icefield?

2) How are changes in the firn impacting hydrology?

First, our measurements suggest that the mean density and liquid water content (LWC) non-monotonically increased through June and July of 2024, which reflects local transient retention of meltwater in the snow and firn during the summer melt season.

Further, model results suggest that firn-column thickness decreased by 16-27% from 1980-2019, with a significant portion occurring since 2012 due to increased negative surface mass balance (i.e., increased melt and decreased snow accumulation).

https://doi.org/10.5194/egusphere-2025-5750
Preprint. Discussion started: 19 January 2026

While highly variable, the cold content in the firn decreased from 1980-2019 (-34 to -48 %) and the number of days with near-zero cold content increased by 2.3-5.3 days per decade. These changes have ultimately led to an increase in meltwater runoff from the firn (48-70%), decrease in meltwater refreeze in the firn (22-36%), and the onset of the runoff season occurring earlier in the year.

4.1 Climate

Across the Juneau Icefield, equilibrium-line altitudes are increasing, causing decreased mass balance (-0.68 $\pm$ 0.15 m w.e. a^{-1} (Berthier et al., 2018) due to increased ablation from rising atmospheric temperatures (Ing et al., 2025), with a doubling of mass loss during the 1979 to 2010 to 2010–2020 time periods (Davies et al., 2024). Specifically, previous studies have shown increases in winter temperature and melt on the icefield (Davies et al., 2024), and widespread trends of increasing temperatures and expanding melt seasons in other regions across Alaska (Blaskey et al., 2023; Winski et al., 2018)) and in the Yukon (Kindstedt et al., 2025). At our three study sites, we identified symptoms of these larger changes: winter temperatures across all three study sites on the Juneau Icefield have been increasing (0.2-0.3 ° C per decade), causing a lengthened melt season (3.8 - 5.8 days per decade). Further, melt is increasing (0.11-0.26 m i.e. per decade), snow accumulation is decreasing (0.11-0.26 m i.e., per decade), with little long-term changes in rainfall, leading to decreased surface mass balance. This has had a variety of implications on the firn of the Juneau Icefield: (1) thinning and disappearance of the firn layer, especially since 2012; (2) a higher-density firn column and decreased firn-air content; and (3) decreased capacity for refreezing and increased runoff. We elaborate on these impacts below.

4.2 Firn changes

Our measurements of LWC in the snow and firn are similar to LWC observations from previous studies for snow on the Juneau Icefield (e.g., volumetric LWC 1.7% – 5.7% in 2012, and 2.1% – 16% in 2021 (Mannello et al., 2025)). Snow studies at other locations find similar magnitudes of LWC, from snow studies using geophysical observations (0-19% vol., Webb et al. (2018); 4-5 % vol., Heilig et al. (2015); and over 10 % vol., Bonnell et al. (2021)), and those using similar measurement devices to this study (i.e., Denoth meter and Snow Fork) in a seasonal snowpack (between 0-10 % vol.; Techel and Pielmeier (2011)). To our knowledge, in-situ measurements of LWC in the firn are non-existent.

We find that the mean density and liquid water content (LWC) non-monotonically increased through June and July of 2024 (Table 3), which reflects local transient retention of meltwater in the snow and firn during the beginning of the melt season; transient processes such as meltwater infiltration and draining into crevasses; and/or spatial variability of water movement due to microstructure and macrostructure (e.g., discontinuous ice lenses). Any transient liquid water that is drained is not captured in the measurements. While the cores were taken within 1-3 meters, spatial variability may contribute to uncertainty in the LWC measurements and comparison from repeat firn cores.

In particular, we infer that there is transient liquid water storage in the snow and firn at the three study sites. Most of the measured LWC is higher than the irreducible water saturation (2-3 %), which implies that the water flux out of the firn is not as rapid as its generation, either because (1) the snow and firn do not have high enough permeability, and/or (2) the hydraulic

https://doi.org/10.5194/egusphere-2025-5750
Preprint. Discussion started: 19 January 2026

head is not high enough to accommodate the meltwater flux into the system. Diurnal, seasonal, and spatial variations in LWC in the snow and firn are a result of variable meltwater processes that control liquid water flux in and out of the snow and firn (e.g., LWC history, snow melt rate, rainfall, snow and firn macro- and microstructure, drainage into crevasses), or variations in slope. Inter-seasonal variability in LWC in the snow through the summer season has also been observed in previous studies on the icefield as well (Mannello et al., 2025).

Some larger stratigraphic layers (e.g., ice layers) observed at the MLD firn-core sites coincide with several surface conformable and apparently continuous bright horizons within the GPR profiles, which suggest that some relatively continuous layers at near-constant depths exist within the snow and firn near the core sites. However, our repeat firn cores that were taken 1-3 m apart, snow-pit observations (not apart of this study), and unstacked radar profiles also reveal numerous discontinuous horizons, suggesting that layering in the snow and firn across the Juneau Icefield is complex. The differences in stratigraphy of each of the repeat firn cores at a single site (Figure 3) highlights that even great spatial variability exists in the snow and firn of high-melt temperate alpine glaciers due to the impacts of snow structures (e.g., sastrugi and wind crusts) and stratigraphic variations (e.g., microstructural and macrostructural layer variations in the snow and firn that translate to differential permeabilities) on snow-melt processes and melt infiltration, on micrometer to meter scales.

For example, we find ice layers and lenses tend to extend across the entire firn core as well as features that do not (e.g., discontinuous ice layers, ice conduits). Horizontal and continuous ice layers may suggest a more homogenous wetting front during melt infiltration that is controlled less by stratigraphic barriers, while ice conduits and discontinuous ice layers suggest preferential flow. Very thin ice layers (< 0.25 cm) that we observe widely in all firn cores may represent surface refreezing instead of meltwater infiltration into the snow and firn (e.g., Kindstedt et al. (2025)). We observe several thick ice layers in the firn (the largest ice layer was 22 cm in core MLD_C3) as well as clusters of thick ice layers in most cores, which may form from repeated, intense, and/or long melt events, and/or be a thick stratigraphic barrier to which subsequent liquid water may refreeze on.

At all three sites, model results suggest that a negative surface mass balance (increasing melt and decreasing snow accumulation) results in firn thinning from 1980-2019. At NWB1, melt actually exceeds accumulation in 2019, which suggests that NWB1 possibly has entered the ablation zone, concurrent with recent icefield-wide ELA increases (Pelto, 2019). As a result of firn thinning, mean firn-column density increased from 1980-2019 (3-5%), firn-air content decreased (21-35%), and consequently mean annual LWC is decreased in the firn column. Increasing firn-column densities are due to increased compaction than increased refreezing, as runoff dominates refreezing, which has been observed at other Alaskan glaciers (Stevens et al., 2024). Factors that also may influence spatial variability of mass balance between sites, and thus firn thickness and thinning on the icefield, include marine proximity and elevation of the site (Mannello, 2023).

4.3 Thermal changes

On the Juneau Icefield, the cold content in the firn governs the capacity of the firn to refreeze meltwater, due to its near-isothermal nature. From 1980–2019, firn cold content in the upper 20 m occurred seasonally, with no retention of cold content between years and full depletion with each early summer. This annual exhaustion contrasts to sites such as interior Greenland,

https://doi.org/10.5194/egusphere-2025-5750
Preprint. Discussion started: 19 January 2026

where a subsurface cold reservoir persists year-round (Vandecrux et al., 2020) and meltwater refreezing in the firn is governed by a variety of factors (e.g., available pore space, cold content, meltwater availability). These cold-content results underscore the limited buffering capacity of warm temperate firn on the Juneau Icefield, and similar glaciers in Alaska, to refreeze meltwater in a warming climate.

As a result of increasing winter temperatures, an increasing melt season, and consequently decreasing firn cold content, the shift a runoff-dominated regime in the firn is initiated earlier in the year (9-19 days from 1980-2019). The runoff and refreeze seasons overlap during late May and early June for the three sites, when there is still enough winter cold content in the upper 3-5 m of the snow/firn column to refreeze liquid water (rain and/or melt) that is introduced in the system as ice layers and other ice features. However, after the melt season progresses and the snow/firn column becomes entirely isothermal, then the regime switches to a fully runoff regime in mid June to early July until the end of the summer melt season in October. While the amount of surface melt increased at 0.11-0.26 m i.e. per decade from 1980-2019, and the percent melt and rain that is runoff from the firn is also increasing (8-12% change), the percent melt that is being refrozen in the firn is decreasing (44-58% change) from 1980-2019. At some sites, runoff and refreeze do not change reversibly, which further shows that transient liquid water storage resides locally in the firn. We expect that due to continued winter warming, increasing melt (i.e., lengthening of the melt season and increase in melt events), decreasing cold content, and increasing ELAs (i.e., transition of more sites from the accumulation to ablation zone), that continued decline of firn cold content, increase in runoff, decrease in refreeze, and an earlier onset of a runoff-dominated regime in the firn will occur.

We note that Young et al. (2021) omitted the firn from their hydrological modeling of the Juneau Icefield and showed that the highest glacier meltwater runoff from the icefield is occurring earlier in the year relative to prior decades, at a rate of 2.5 days per decade. While our results are in agreement, in that the melt season onset is earlier in the year, we do not find a significant trend in peak runoff from the firn.

4.4 Aquifers

Liquid water storage in the firn ('firn aquifer') may occur if melt or rainfall input to temperate firn is greater than the rate of evacuation of that liquid water, causing the irreducible water saturation (2-3% vol) of the firn to be surpassed and liquid water to be temporarily stored. Previous studies in Greenland show that firn aquifers contain between 5-25 % vol liquid water (Koenig et al., 2014) that may persist seasonally to perennially. In particular, seasonal late summer/early autumn firn aquifers have been documented in high-accumulation and high-melt regions of temperate alpine glaciers such as in the Oetztal Alps in Austria, Storglaciären in Sweden, and South Cascade Glacier in the United States (Fountain, 1989; Fountain and Walder, 1998; Jansson et al., 2003; Oerter and Rauert, 1982; Schneider, 1999). We suggest that seasonal aquifers in the snow and firn occur locally to regionally in the accumulation zone of the Juneau Icefield during times of high melt, and even during the beginning of the melt season, based on: (1) our LWC measurements (from 10-30 % vol), which exceeds the irreducible water content and is within and greater than the observed range of aquifer LWC values in Greenland; (2) LWC and density observations show increases through June and transient liquid-water retention; and (3) modeled results show interannual liquid-water retention at all sites (> 10 % vol). Determining the timing and persistence of these transient local aquifers on the Juneau Icefield through the rest of

https://doi.org/10.5194/egusphere-2025-5750
Preprint. Discussion started: 19 January 2026

the summer season and interannually, and their spatial occurrence on the icefield, is challenging to assess due to the spatial and temporal limitations of our measurements. However, our modeling results suggest that local liquid water storage may persist between melt seasons. This potentially widespread transient liquid water storage (regardless of whether it is technically a 'firn aquifer' or not) is not only important to consider for mass-balance related calculations (including for geodetic mass-balance estimates and for accurate corrections to ground-penetrating radar velocities used to estimate of SWE (e.g., Stevens et al. (2024); Mannello et al. (2025)), but also for understanding hydrological controls on ice dynamics (e.g., from continuous or episodic drainage through crevasses).

4.5 Broader Impacts

The Taku Glacier is one of the the main outlet glaciers of the Juneau Icefield. Because a significant area (approximately 83%) of the Taku Glacier of the Juneau Icefield lies on the low-slope plateau in the accumulation zone and firn zone (Pelto et al., 2013), we suggest that our results apply to the majority of the Taku Glacier and most likely other locations in the accumulation zone of the Juneau Icefield. We suggest that significant decrease in refreeze capacity and increased runoff in recent years has occurred and will continue to occur across the accumulation zone of the Taku Glacier and possibly the greater Juneau Icefield.

To contextualize our results, we perform an idealized calculation to determine the change in flux from the Taku Glacier into the Taku River drainage. If we consider (a) changes in firn runoff from our modeling results at the three sites in the accumulation zone from 1980-2019; (b) the accumulation area of the Taku Glacier (558 km^2; Pelto et al. (2013)); (c) the area-averaged ablation rate (0.83 m w.e. yr^{-1}; McNeil et al. (2020)); and (d) the area of the Taku Glacier (725 km^2; McNeil et al. (2020)), we estimate that the change in firn runoff from the Taku Glacier increased 2.1-4.4 $\times$ 10^8 m^3 i.e from 1980-2019, which is approximately 45-72% of the total ablation for the Taku Glacier. While there is significant uncertainty associated with this idealized calculation, it generally highlights the capacity of the firn to modulate downstream hydrology, and the importance of shifts in the firn hydrological regime to cause evolution of downstream hydrological changes on the Juneau Icefield and other similar temperate alpine glacier systems.

We suggest that increased runoff from the firn will result in 'flashier' downstream hydrology, where melt and/or rain events are more promptly propagated downstream than if most of the liquid water was refrozen and/or retained as liquid in the firn as ice or liquid. While some liquid water input (rain and melt) is accommodated by refreezing and transient liquid water storage (but is decreasing), the percent that is runoff from the firn is increasing ubiquitously across all sites. In general, flashy hydrological systems may lead to flooding or highly variable stream flow. On the Juneau Icefield, earlier shifts of runoff into downstream environments may cause changes in stream temperature and clarity, and consequently may impact species, such as salmon, that prefer certain freshwater conditions (Young et al., 2021). As ELAs continue to increase and warming firn continues, we expect that firn runoff will continue to dominate firn hydrological processes, and continue to result in a flashy hydrological system that accommodates melt rapidly.

Future icefield-wide increases in atmospheric temperature will cause increasing surface melt and rising ELAs, which will prompt accelerated mass loss due to hypsometrically controlled feedbacks because of the plateau-like nature of the Juneau Icefield (Ing et al., 2025; Davies et al., 2024). We suggest that these continued and accentuated changes will continue to

https://doi.org/10.5194/egusphere-2025-5750
Preprint. Discussion started: 19 January 2026

deplete the firn, decrease the firn cold content, and increase firn runoff. Warming firn and decreased firn capacity for refreezing of liquid water has also occurred in other regions across the temperate Arctic, including in Svalbard, on the Penny Ice Cap (Baffin Island), and on Eclipse Icefield (Yukon) (Noël et al., 2020, 2018; Kindstedt et al., 2025). Firn warming is less reversible than firn cooling, due to the nonlinear effects of temperature on firn-densification processes, which is especially accentuated by latent-heat release due to meltwater refreezing (Thompson-Munson et al., 2024). Therefore, regenerating cold content from locations such as the Juneau Icefield, where long-term firn warming is occurring, is limited.

Understanding spatiotemporal variability of internal accumulation in the firn (i.e., liquid water storage from rain and melt, and refreezing) is fundamental to (1) accurate calculations of mass balance from geodetic methods, a common method to assess mass change on alpine glaciers that often uses a uniform correction factor for volume to mass conversion (Huss, 2013; Stevens et al., 2024); (2) accurate SWE estimates derived from GPR, as liquid water changes impacts the radar-wave velocity and therefore the correction of travel time to depth (e.g., Mannello et al. (2025)); and (3) ice dynamics due to the potential for continuous or episodic draining of liquid water into crevasses. On the icefield, we suggest that transient liquid water and firn aquifers may store significant mass that is not accounted for in the density assumptions from volume to mass conversions and may possibly complicate geodetic mass balance calculations that are not based at the end of the summer season. As Alaskan alpine glaciers continue to experience atmospheric warming, it is important to account meltwater processes in the firn in geodetic mass-balance to derive accurate estimates of sea-level rise (Stevens et al., 2024). Further, uncertainty in radar-derived depth can introduce large uncertainties (up to 45 %) in SWE calculations (Mannello et al., 2025). Increasingly earlier onset of the melt season confirm results from Mannello et al. (2025), which suggested that radar-derived SWE estimates should consider the spatiotemporal variability of liquid water content in the snow even during spring surveys of the Juneau Icefield. Finally, the timscales of the drainage of firn aquifers and other transient liquid water storage (whether episodic or continuous) in the snow and firn is currently unknown, and may impact downglacier seasonal ice-velocity fluctuations on the icefield and at other temperate Alaskan glaciers with high melt.

4.6 Future work

While the Juneau Icefield is currently one of the most studied glacier systems in the world, there remains a lack of measurements spanning the entire firn column. This study is the first to characterize the evolution of the icefield's firn properties and hydrology. However, our study has spatial and temporal limitations, as it focuses primarily on the firn evolution at four sites, with field data collected in June and July of 2024 and modeling extending from 1980-2019. Therefore, further investigation of the spatial and temporal variability of the firn on the Juneau Icefield is needed, in particular: (1) in-situ measurements during a full summer season; and (2) more measurements across the icefield to constrain spatial variability.

In general, we suggest that continued understanding of the evolution of firn on temperate alpine glaciers in Alaska is needed, including understanding of the heterogeneity of meltwater processes. Due to the lack of field measurements and limitations of point measurements, firn models are commonly used to determine firn evolution over wide spatiotemporal scales. Improvement of these models also requires more observations of microstructural properties (e.g., grain size and permeability) Vandecrux et al. (2020) and associated meltwater processes.

https://doi.org/10.5194/egusphere-2025-5750
Preprint. Discussion started: 19 January 2026

5 Conclusions

Alaskan glaciers currently contribute 25 % of the global land-ice loss to sea-level rise and, due to continued atmospheric warming, are expected to remain a principal contributor at least through the end of the century. Most Alaskan glaciers lose mass through surface melting, which is routed through the firn and may be stored temporarily as liquid or ice, or run off downstream. Here, we use field observations and firn modeling to investigate seasonal to decadal changes in the thermal and physical properties of firn on the Juneau Icefield, Alaska. Firstly, we find that mean density and liquid water content generally increase up to 5%and 71 %, respectively, through the beginning of the 2024 summer season, which suggests seasonal transient retention of meltwater. From 1980-2019, we find that due to increasing atmospheric temperatures, increasing surface melt, and decreasing snow accumulation, the firn-air content decreased between 22% to 35% due to decreasing firn thickness and increasing firn densities. Finally, we find that the firn cold content decreased from 1980-2019, causing increasing meltwater runoff from the firn (63% to 76%), decreased meltwater refreeze (-24 to -39%), and shift of the refreeze and runoff transition 7-18 days earlier in the season due to increasing surface melt and decreasing snow accumulation. We suggest that potentially widespread transient local liquid water storage occurs widely across the icefield, and that some of these areas with high LWC (> irreducible water saturation, 2-3 % vol, and up to 30 % vol) may be transient seasonal aquifers in the snow and firn. Our results suggest that firn on the Juneau Icefield and other temperate alpine glaciers of Alaska will continue to lose long-term meltwater refreezing capacity, while increasing firn runoff may continue to promote flashy downstream hydrology. In addition, inter-seasonal shifts in liquid water retention may introduce uncertainties in mass-balance calculations for sea-level rise estimates. Future studies should consider additional firn measurements across the Juneau Icefield and other temperate Alaskan glaciers to further constrain spatiotemporal variability of meltwater impacts on firn evolution in the context of a warming climate.

https://doi.org/10.5194/egusphere-2025-5750
Preprint. Discussion started: 19 January 2026

Appendix A

A1

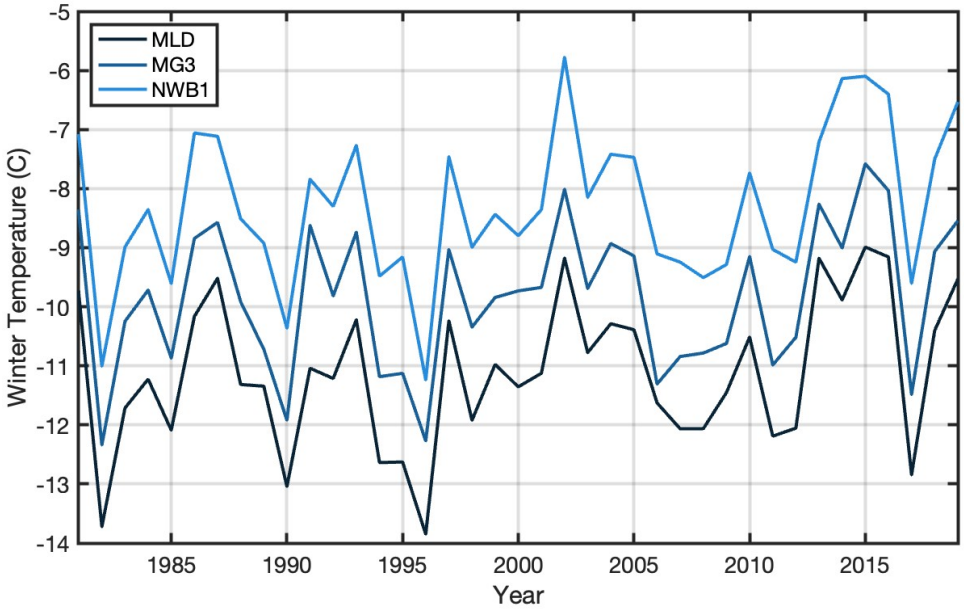

Figure A1. Mean annual winter temperatures for the three accumulation-zone sites, derived from Ing et al. (2025)

https://doi.org/10.5194/egusphere-2025-5750
Preprint. Discussion started: 19 January 2026

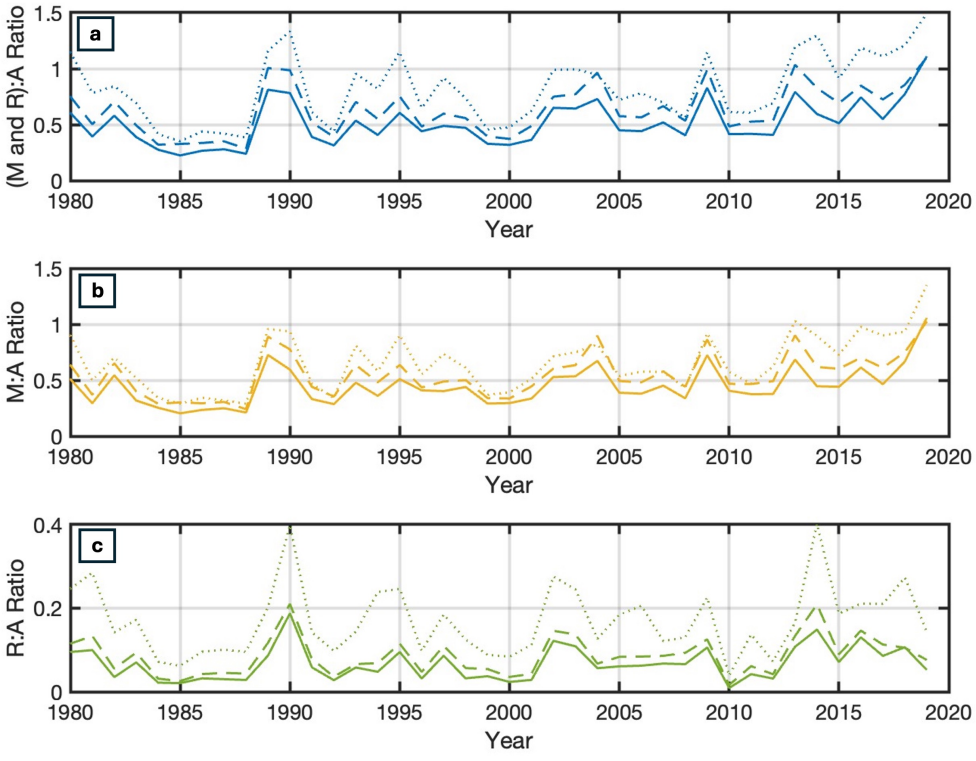

Figure A2. Comparison between climate variables from Ing et al. (2025) for the three accumulation-zone sites (MLD, dotted line; MG3, dashed line; NWB1, solid line). a) Ratio between the sum of cumulative annual melt and rain to the cumulative annual snow accumulation; b) ratio between melt and accumulation; c) ratio between rain and accumulation.

https://doi.org/10.5194/egusphere-2025-5750
Preprint. Discussion started: 19 January 2026

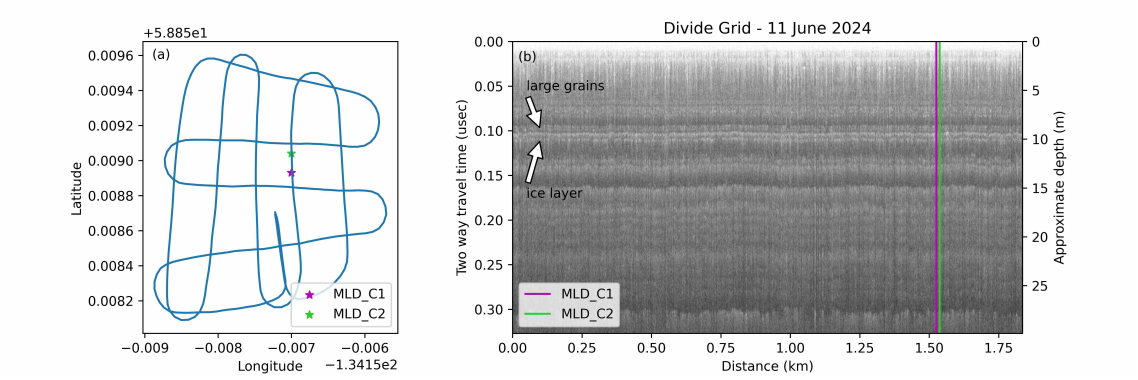

Figure A3. GPR grid at MLD and interpretations of semi-continuous layering that is in agreement with core measurements. Core locations relative to the radargrams are denoted by stars (a) and vertical lines (b).

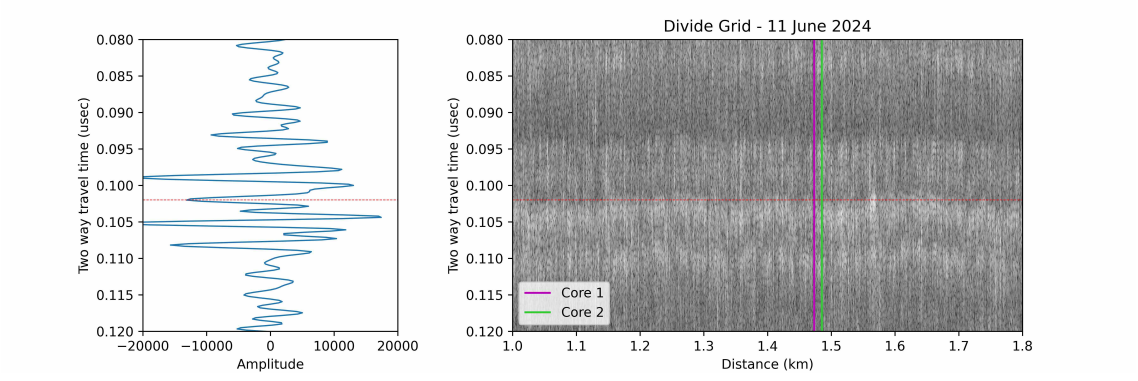

Figure A4. Zoomed in view of (a) oscilloscope of (b) GPR grid at MLD on June 11 2024 of identified layer in Figure A3 where it intersects with the core.

https://doi.org/10.5194/egusphere-2025-5750
Preprint. Discussion started: 19 January 2026

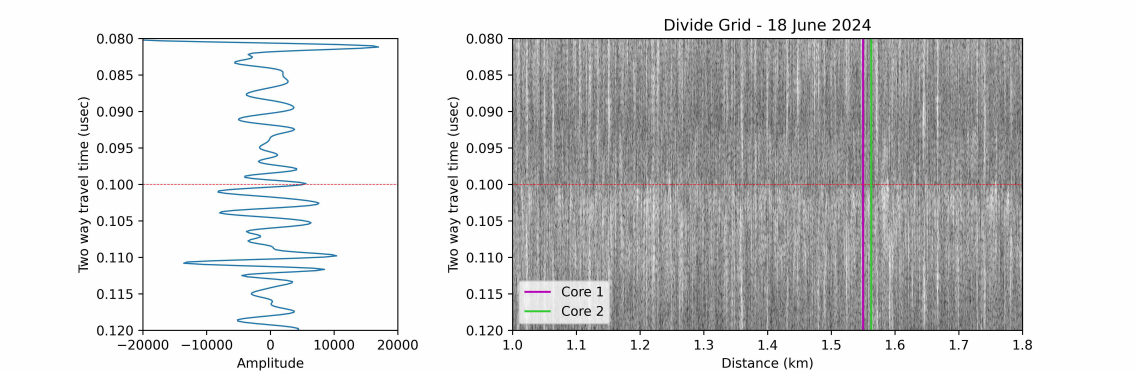

Figure A5. Zoomed view of (a) oscilloscope of (b) GPR grid at MLD on June 18 2024 of identified layer in Figure A3 where it intersects with the core.

https://doi.org/10.5194/egusphere-2025-5750
Preprint. Discussion started: 19 January 2026

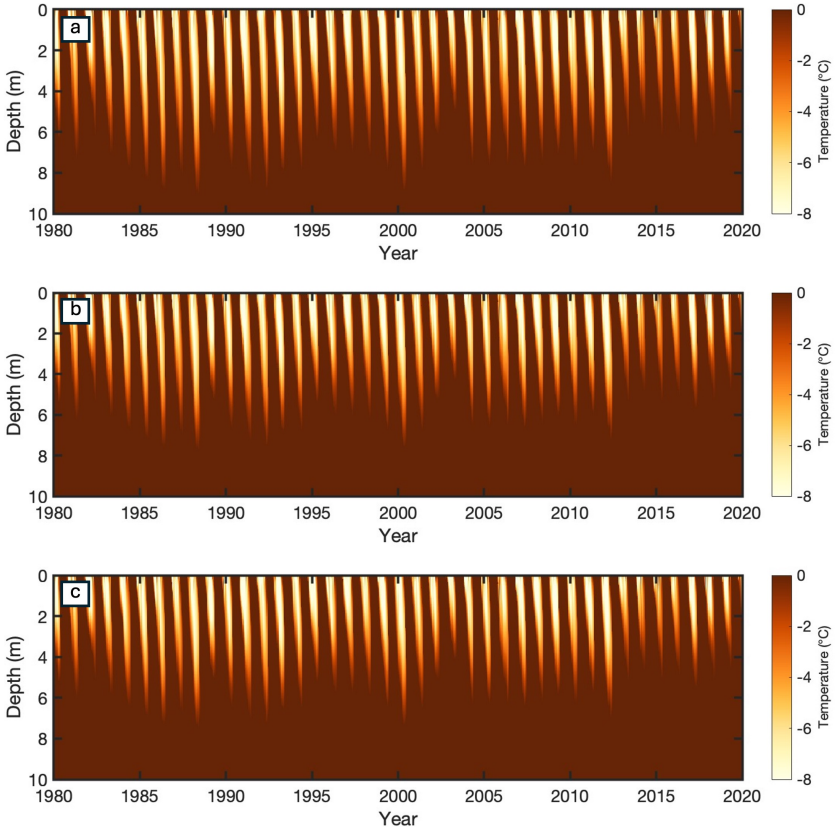

Figure A6. Modeled firn temperature profiles from 1980-2019 for a) MLD; b) MG3; c) NWB1.

https://doi.org/10.5194/egusphere-2025-5750
Preprint. Discussion started: 19 January 2026

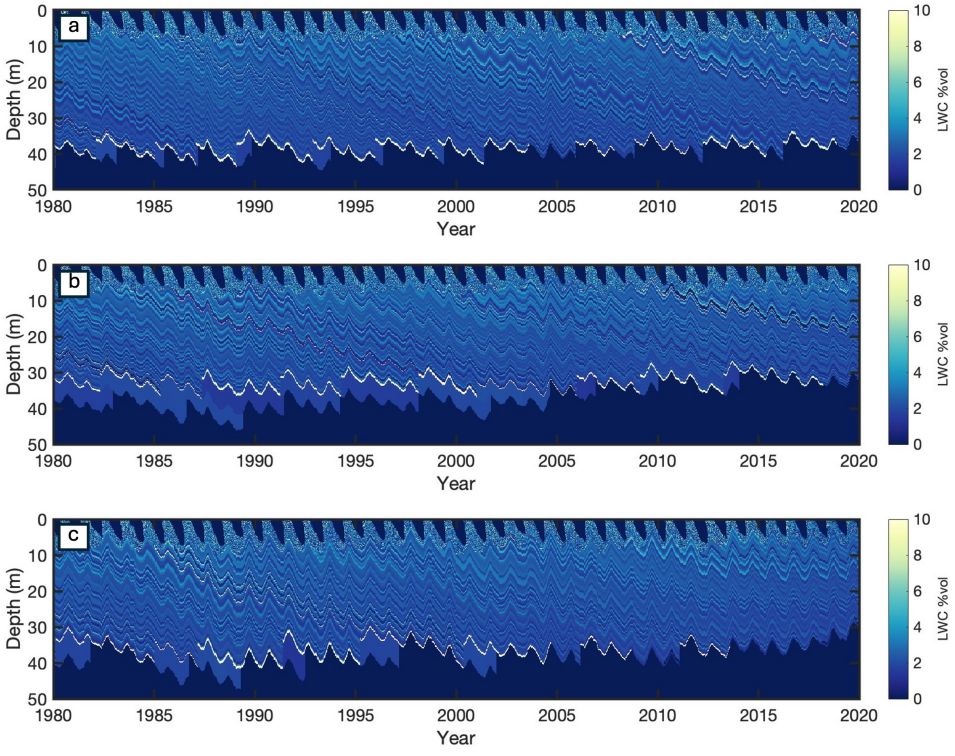

Figure A7. Modeled liquid-water content (LWC) evolution for the three sites: a) MLD, b) MG3, and c) NWB1.

https://doi.org/10.5194/egusphere-2025-5750
Preprint. Discussion started: 19 January 2026

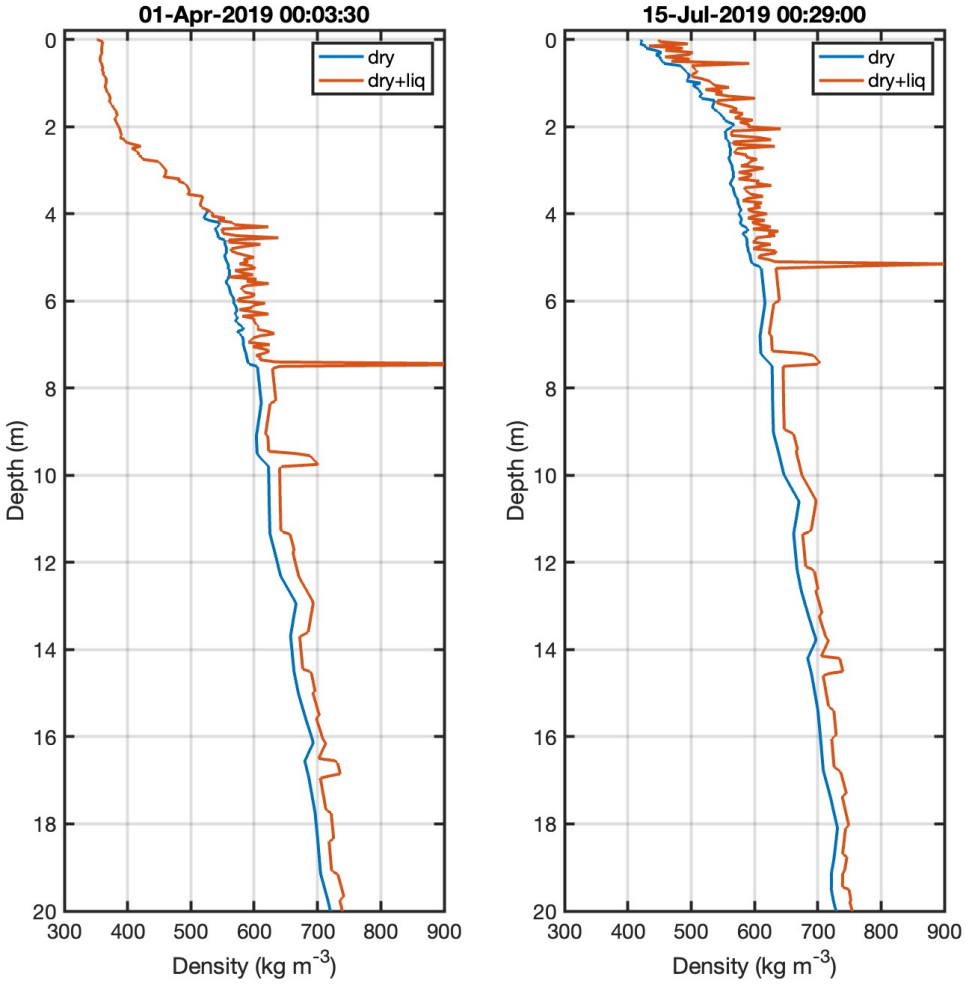

Figure A8. Modeled depth-density profiles for April and July of 2019 at Site MLD, showing the ablation of the snow layer, and the dry and wet densities.

https://doi.org/10.5194/egusphere-2025-5750
Preprint. Discussion started: 19 January 2026

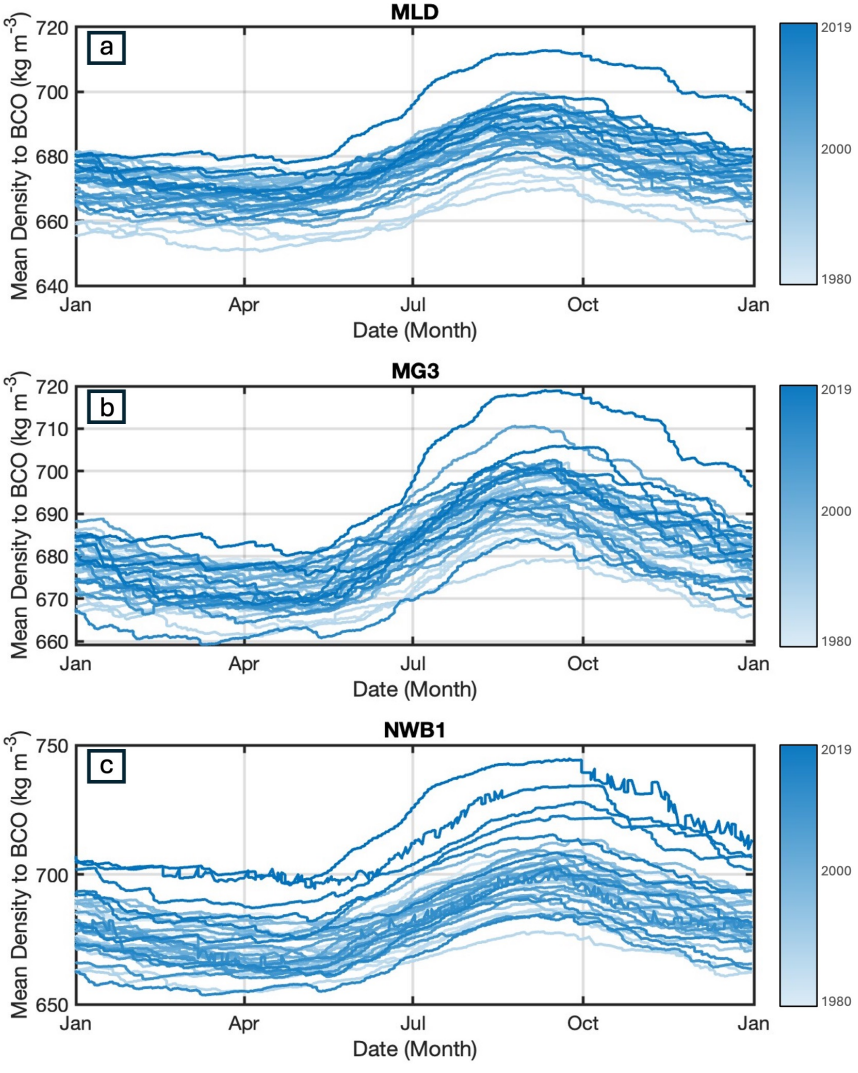

Figure A9. Modeled seasonal mean density (dry + liquid) from 1980-2019 for the three sites: a) MLD, b) MG3, and c) NWB1.

https://doi.org/10.5194/egusphere-2025-5750
Preprint. Discussion started: 19 January 2026

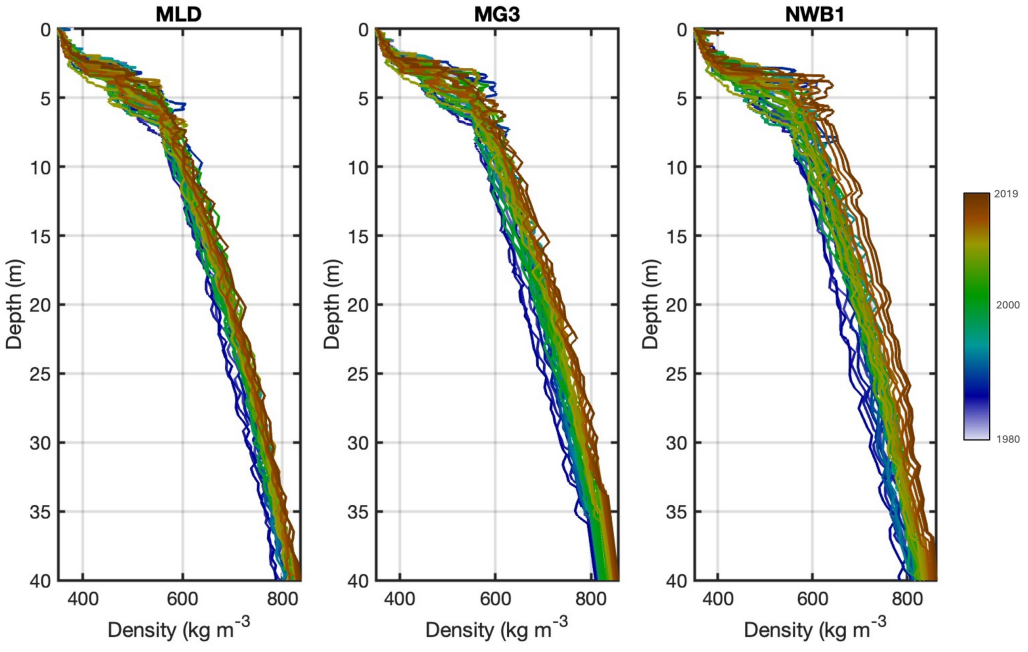

Figure A10. Modeled mean annual density (dry + liquid) profiles from 1980-2019 for the three sites: a) MLD, b) MG3, and c) NWB1.

https://doi.org/10.5194/egusphere-2025-5750
Preprint. Discussion started: 19 January 2026

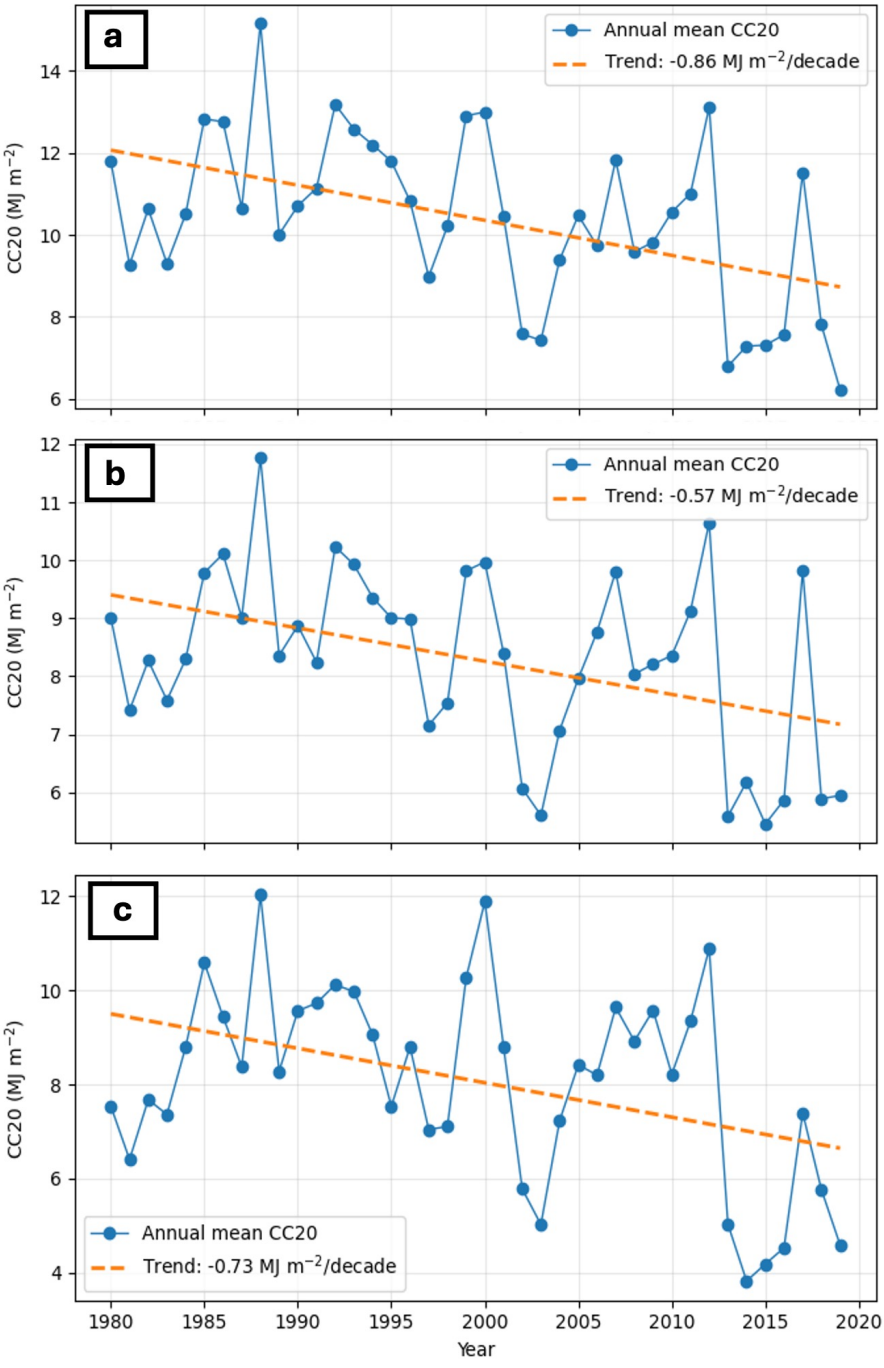

Figure A11. Mean annual cold content calculated from model results from 1980-2019 for the three sites: a) MLD, b) MG3, and c) NWB1.

https://doi.org/10.5194/egusphere-2025-5750
Preprint. Discussion started: 19 January 2026

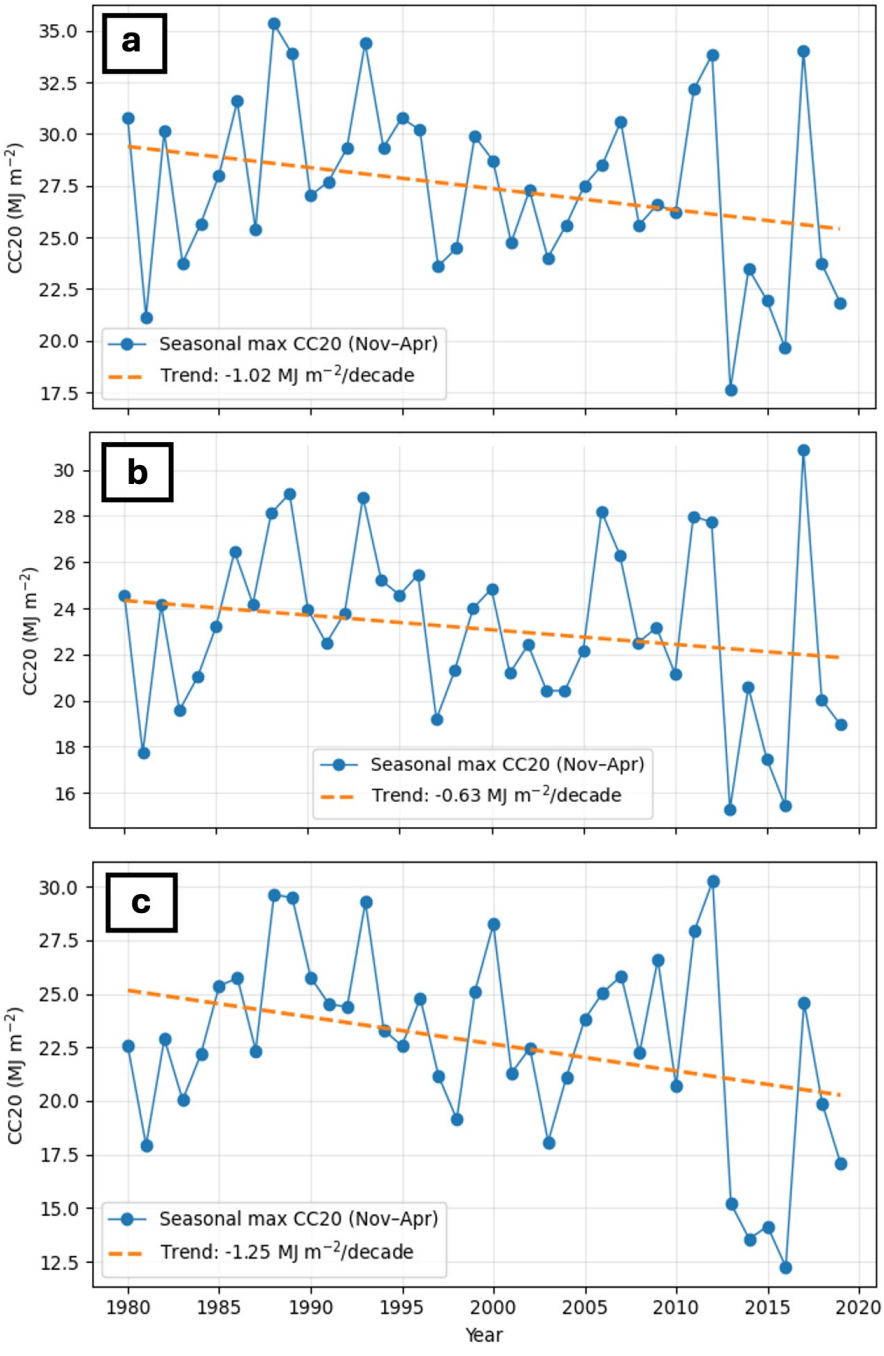

Figure A12. Mean winter cold content (Nov-Apr) calculated from model results from 1980-2019 for the three sites: a) MLD, b) MG3, and c) NWB1.

https://doi.org/10.5194/egusphere-2025-5750
Preprint. Discussion started: 19 January 2026

Code and data availability. The CFM code is publicly available at https://github.com/UWGlaciology/CommunityFirnModel. Documentation for the CFM is online at https://communityfirnmodel.readthedocs.io/TS5. Firn-core data and firn-model output are available through the NSF Arctic Data Center at: https://arcticdata.io/catalog/view/doi%3A10.18739%2FA22V2CC52. All outputs from this study are also available from the authors without conditions.

Author contributions. A.N.H conceptualized the study with the mentorship of B.M. A.N.H. led the field season and A.N.H, J.R., B.M., M.M., K.B., T.W. collected the firn cores. S.C. provided the field equipment. M.M. and K.B. collected GPR and conceptualized Wise-sensor measurements. A.N.H. performed analysis and interpretation of field and climate data, led modeling and interpretation, and wrote the manuscript. C.M.S. contributed to modeling and interpretations. J.R. performed cold-content calculations. J.R., C.M.S., M.M., K.B., and T.W. contributed to writing. All authors contributed to editing of the manuscript.

Competing interests. The authors declare they have no conflict of interest.

Acknowledgements. We thank the Juneau Icefield Research Program (JIRP) for field support. We also are grateful to Lynn Brennan, Erin Towns, and Mari Fromstein for their help in the field. This work was supported by National Science Foundation Office of Polar Programs Postdoctoral Award #2318348; NSF Career Grant #2239668; and Army contract W913E523C0003.

https://doi.org/10.5194/egusphere-2025-5750
Preprint. Discussion started: 19 January 2026

References

Ashmore, D. W., Mair, D. W., and Burgess, D. O.: Meltwater percolation, impermeable layer formation and runoff buffering on Devon Ice Cap, Canada, Journal of Glaciology, 66, 61–73, 2020.

Berthier, E., Larsen, C., Durkin, W. J., Willis, M. J., and Pritchard, M. E.: Brief communication: Unabated wastage of the Juneau and Stikine icefields (southeast Alaska) in the early 21st century, The Cryosphere, 12, 1523–1530, 2018.

Blaskey, D., Koch, J. C., Gooseff, M. N., Newman, A. J., Cheng, Y., O'Donnell, J. A., and Musselman, K. N.: Increasing Alaskan river discharge during the cold season is driven by recent warming, Environmental Research Letters, 18, 024 042, 2023.

Bonnell, R., McGrath, D., Williams, K., Webb, R., Fassnacht, S. R., and Marshall, H.-P.: Spatiotemporal variations in liquid water content in a seasonal snowpack: implications for radar remote sensing, Remote Sensing, 13, 4223, 2021.

Clerx, N., Machguth, H., Tedstone, A., Jullien, N., Wever, N., Weingartner, R., and Roessler, O.: In situ measurements of meltwater flow through snow and firn in the accumulation zone of the SW Greenland Ice Sheet, The Cryosphere, 16, 4379–4401, 2022.

Colbeck, S.: Water flow through snow overlying an impermeable boundary, Water Resources Research, 10, 119–123, 1974.

Coléou, C. and Lesaffre, B.: Irreducible water saturation in snow: experimental results in a cold laboratory, Annals of glaciology, 26, 64–68, 1998.

Consortium, R. et al.: Randolph glacier inventory-a dataset of global glacier outlines, version 7, NASA National Snow and Ice Data Center Distributed Active Archive Center (DAAC) data set, p. F6JMOVY5NAVZ, 2023.

Culberg, R., Schroeder, D. M., and Chu, W.: Extreme melt season ice layers reduce firn permeability across Greenland, Nature communications, 12, 2336, 2021.

Davies, B., McNabb, R., Bendle, J., Carrivick, J., Ely, J., Holt, T., Markle, B., McNeil, C., Nicholson, L., and Pelto, M.: Accelerating glacier volume loss on Juneau Icefield driven by hypsometry and melt-accelerating feedbacks, Nature Communications, 15, 5099, 2024.

Forster, R. R., Box, J. E., Van Den Broeke, M. R., Miège, C., Burgess, E. W., Van Angelen, J. H., Lenaerts, J. T., Koenig, L. S., Paden, J., Lewis, C., et al.: Extensive liquid meltwater storage in firn within the Greenland ice sheet, Nature Geoscience, 7, 95–98, 2014.

Fountain, A. G.: The storage of water in, and hydraulic characteristics of, the firn of South Cascade Glacier, Washington State, USA, Annals of Glaciology, 13, 69–75, 1989.

Fountain, A. G.: Effect of snow and firn hydrology on the physical and chemical characteristics of glacial runoff, Hydrological Processes, 10, 509–521, 1996.

Fountain, A. G. and Walder, J. S.: Water flow through temperate glaciers, Reviews of geophysics, 36, 299–328, 1998.

Fox-Kemper, B., Hewitt, H., Xiao, C., Aðalgeirsdóttir, G., Drijfhout, S., Edwards, T., Golledge, N., Hemer, M., Kopp, R., Krinner, G., et al.: Ocean, cryosphere and sea level change. Climate change 2021: the physical science basis. Contribution of Working Group I to the Sixth Assessment Report of the Intergovernmental Panel on Climate Change, Climate Change, 2021.

Heilig, A., Mitterer, C., Schmid, L., Wever, N., Schweizer, J., Marshall, H.-P., and Eisen, O.: Seasonal and diurnal cycles of liquid water in snow—Measurements and modeling, Journal of Geophysical Research: Earth Surface, 120, 2139–2154, 2015.

Hirashima, H., Avanzi, F., and Wever, N.: Wet-snow metamorphism drives the transition from preferential to matrix flow in snow, Geophysical Research Letters, 46, 14 548–14 557, 2019.

Hock, R., Rasul, G., Adler, C., Cáceres, B., Gruber, S., Hirabayashi, Y., Jackson, M., Kääb, A., Kang, S., Kutuzov, S., et al.: High mountain areas, in: IPCC special report on the ocean and cryosphere in a changing climate, pp. 131–202, H.-O. Pörtner, DC Roberts, V. Masson-Delmotte, P. Zhai, M. Tignor, E . . . , 2019.

https://doi.org/10.5194/egusphere-2025-5750
Preprint. Discussion started: 19 January 2026

Horlings, A. N., Christianson, K., and Miège, C.: Expansion of firn aquifers in southeast Greenland, Journal of Geophysical Research: Earth Surface, 127, e2022JF006 753, 2022.

Hugonnet, R., McNabb, R., Berthier, E., Menounos, B., Nuth, C., Girod, L., Farinotti, D., Huss, M., Dussaillant, I., Brun, F., et al.: Accelerated global glacier mass loss in the early twenty-first century, Nature, 592, 726–731, 2021.

Humphrey, N. F., Harper, J. T., and Meierbachtol, T. W.: Physical limits to meltwater penetration in firn, Journal of Glaciology, 67, 952–960, 2021.

Huss, M.: Density assumptions for converting geodetic glacier volume change to mass change, The Cryosphere, 7, 877–887, 2013.

Ing, R. N., Ely, J. C., Jones, J. M., and Davies, B. J.: Surface mass balance modelling of the Juneau Icefield highlights the potential for rapid ice loss by the mid-21st century, Journal of Glaciology, 71, e11, 2025.

Jansson, P., Hock, R., and Schneider, T.: The concept of glacier storage: a review, Journal of Hydrology, 282, 116–129, 2003.

Kindstedt, I., Winski, D., Stevens, C. M., Skelton, E., Copland, L., Kreutz, K., Mannello, M., Clavette, R., Holmes, J., Albert, M., et al.: Ongoing firn warming at Eclipse Icefield, Yukon, indicates potential widespread meltwater percolation and retention in firn pack across the St. Elias Range, The Cryosphere, 19, 3655–3680, 2025.

Koenig, L. S., Miège, C., Forster, R. R., and Brucker, L.: Initial in situ measurements of perennial meltwater storage in the Greenland firn aquifer, Geophysical Research Letters, 41, 81–85, 2014.

Kuipers Munneke, P., Ligtenberg, S., Noël, B., Howat, I., Box, J., Mosley-Thompson, E., McConnell, J., Steffen, K., Harper, J., Das, S., et al.: Elevation change of the Greenland Ice Sheet due to surface mass balance and firn processes, 1960–2014, The Cryosphere, 9, 2009–2025, 2015.

Larsen, C., Burgess, E., Arendt, A., O'neel, S., Johnson, A., and Kienholz, C.: Surface melt dominates Alaska glacier mass balance, Geophysical Research Letters, 42, 5902–5908, 2015.

Lilien, D. A., Hills, B. H., Driscol, J., Jacobel, R., and Christianson, K.: ImpDAR: an open-source impulse radar processor, Annals of Glaciology, 61, 114–123, 2020.

Machguth, H., MacFerrin, M., van As, D., Box, J. E., Charalampidis, C., Colgan, W., Fausto, R. S., Meijer, H. A., Mosley-Thompson, E., and van de Wal, R. S.: Greenland meltwater storage in firn limited by near-surface ice formation, Nature Climate Change, 6, 390–393, 2016.

Machguth, H., Tedstone, A. J., and Mattea, E.: Daily variations in Western Greenland slush limits, 2000–2021, Journal of Glaciology, 69, 191–203, 2023.

Mannello, M.: Spatial and Temporal Variability in Snow Properties and Firn Volume Across the Juneau Icefield in Southeast Alaska, The University of Maine, 2023.

Mannello, M. A., Braddock, S., Campbell, S. W., Skelton, E., Schild, K. M., and McNeil, C.: Constraining snow water equivalent of wet snowpacks in Southeast Alaska, Annals of Glaciology, 66, e21, 2025.

McDowell, I. E., Keegan, K. M., Wever, N., Osterberg, E. C., Hawley, R. L., and Marshall, H.-P.: Firn Core Evidence of Two-Way Feedback Mechanisms Between Meltwater Infiltration and Firn Microstructure From the Western Percolation Zone of the Greenland Ice Sheet, Journal of Geophysical Research: Earth Surface, 128, e2022JF006 752, 2023.

McNeil, C., O'Neel, S., Loso, M., Pelto, M., Sass, L., Baker, E. H., and Campbell, S.: Explaining mass balance and retreat dichotomies at Taku and Lemon Creek Glaciers, Alaska, Journal of Glaciology, 66, 530–542, 2020.

https://doi.org/10.5194/egusphere-2025-5750
Preprint. Discussion started: 19 January 2026

Miller, O., Solomon, D. K., Miège, C., Koenig, L., Forster, R., Schmerr, N., Ligtenberg, S. R., Legchenko, A., Voss, C. I., Montgomery, L., et al.: Hydrology of a perennial firn aquifer in Southeast Greenland: an overview driven by field data, Water Resources Research, 56, e2019WR026 348, 2020.

Moser, D. E., Thomas, E. R., Nehrbass-Ahles, C., Eichler, A., and Wolff, E.: Melt-affected ice cores for polar research in a warming world, The Cryosphere, 18, 2691–2718, 2024.

Noël, B., Van De Berg, W. J., Lhermitte, S., Wouters, B., Schaffer, N., and van den Broeke, M. R.: Six decades of glacial mass loss in the Canadian Arctic Archipelago, Journal of Geophysical Research: Earth Surface, 123, 1430–1449, 2018.

Noël, B., Jakobs, C. L., Van Pelt, W., Lhermitte, S., Wouters, B., Kohler, J., Hagen, J. O., Luks, B., Reijmer, C., Van de Berg, W. J., et al.: Low elevation of Svalbard glaciers drives high mass loss variability, Nature Communications, 11, 4597, 2020.

Ochwat, N. E., Marshall, S. J., Moorman, B. J., Criscitiello, A. S., and Copland, L.: Evolution of the firn pack of Kaskawulsh Glacier, Yukon: meltwater effects, densification, and the development of a perennial firn aquifer, The Cryosphere, 15, 2021–2040, 2021.

Oerter, H. and Rauert, W.: Core drilling on Vernagtferner (Oetztal Alps, Austria) in 1979: tritium contents, Zeitschrift für Gletscherkunde und Glazialgeologie, 1, 13–22, 1982.

Pelto, M.: Exceptionally high 2018 equilibrium line altitude on Taku Glacier, Alaska, Remote Sensing, 11, 2378, 2019.

Pelto, M., Kavanaugh, J., and McNeil, C.: Juneau icefield mass balance program 1946–2011, Earth System Science Data, 5, 319–330, 2013.

Poinar, K., Joughin, I., Lilien, D., Brucker, L., Kehrl, L., and Nowicki, S.: Drainage of Southeast Greenland firn aquifer water through crevasses to the bed, Frontiers in Earth Science, 5, 5, 2017.

Saha, S., Moorthi, S., Pan, H.-L., Wu, X., Wang, J., Nadiga, S., Tripp, P., Kistler, R., Woollen, J., Behringer, D., et al.: The NCEP climate forecast system reanalysis, Bulletin of the American Meteorological Society, 91, 1015–1058, 2010.

Schneider, T.: Water movement in the firn of Storglaciären, Sweden, Journal of Glaciology, 45, 286–294, 1999.

Schneider, T. and Jansson, P.: Internal accumulation in firn and its significance for the mass balance of Storglaciären, Sweden, Journal of Glaciology, 50, 25–34, 2004.

Shadab, M. A., Adhikari, S., Rutishauser, A., Grima, C., and Hesse, M. A.: A mechanism for ice layer formation in glacial firn, Geophysical Research Letters, 51, e2024GL109 893, 2024.

Stevens, C. M., Verjans, V., Lundin, J. M., Kahle, E. C., Horlings, A. N., Horlings, B. I., and Waddington, E. D.: The community firn model (cfm) v1. 0, Geoscientific Model Development Discussions, 2020, 1–37, 2020.

Stevens, C. M., Sass, L., Florentine, C., McNeil, C., Baker, E., and Bollen, K.: Direct measurements of firn-density evolution from 2016 to 2022 at Wolverine Glacier, Alaska, Journal of Glaciology, 70, e2, 2024.

Techel, F. and Pielmeier, C.: Point observations of liquid water content in wet snow–investigating methodical, spatial and temporal aspects, The Cryosphere, 5, 405–418, 2011.

The Firn Symposium Team: Firn on ice sheets, Nature Reviews Earth & Environment, 5, 79–99, 2024.

Thompson-Munson, M., Kay, J. E., and Markle, B. R.: Greenland's firn responds more to warming than to cooling, The Cryosphere, 18, 3333–3350, 2024.

Vandecrux, B., Mottram, R., Langen, P. L., Fausto, R. S., Olesen, M., Stevens, C. M., Verjans, V., Leeson, A., Ligtenberg, S., Kuipers Munneke, P., et al.: The firn meltwater Retention Model Intercomparison Project (RetMIP): evaluation of nine firn models at four weather station sites on the Greenland ice sheet, The Cryosphere, 14, 3785–3810, 2020.

Webb, R., Jennings, K., Fend, M., and Molotch, N.: Combining ground-penetrating radar with terrestrial LiDAR scanning to estimate the spatial distribution of liquid water content in seasonal snowpacks, Water Resources Research, 54, 10–339, 2018.

https://doi.org/10.5194/egusphere-2025-5750
Preprint. Discussion started: 19 January 2026

Webb, R. W., Marziliano, A., McGrath, D., Bonnell, R., Meehan, T. G., Vuyovich, C., and Marshall, H.-P.: In situ determination of dry and wet snow permittivity: Improving equations for low frequency radar applications, Remote Sensing, 13, 4617, 2021.

Winski, D., Osterberg, E., Kreutz, K., Wake, C., Ferris, D., Campbell, S., Baum, M., Bailey, A., Birkel, S., Introne, D., et al.: A 400-year ice core melt layer record of summertime warming in the Alaska Range, Journal of Geophysical Research: Atmospheres, 123, 3594–3611, 2018.

Young, J. C., Pettit, E., Arendt, A., Hood, E., Liston, G. E., and Beamer, J.: A changing hydrological regime: Trends in magnitude and timing of glacier ice melt and glacier runoff in a high latitude coastal watershed, Water Resources Research, 57, e2020WR027 404, 2021.

Ziemen, F. A., Hock, R., Aschwanden, A., Khroulev, C., Kienholz, C., Melkonian, A., and Zhang, J.: Modeling the evolution of the Juneau Icefield between 1971 and 2100 using the Parallel Ice Sheet Model (PISM), Journal of Glaciology, 62, 199–214, 2016.